

The effect of *Nampt* overexpression on cellular senescence

(細胞老化に対する *Nampt* 高発現の効果)

Figri Dizar bin Khaidizar

Laboratory of Gene Regulation Research

Nara Institute of Science and Technology

Graduate School of Biological Sciences

(Prof. Yasumasa Bessho)

Submitted on 2017/10/31

Lab name (Supervisor)	Gene Regulation Research Laboratory (Prof. Yasumasa Bessho)		
Name (surname) (given name)	Khaidizar, Figri Dizar	Date	17/10/31
Title	The effect of <i>Nampt</i> overexpression on cellular senescence (細胞老化に対する <i>Nampt</i> 高発現の効果)		
<p>Abstract</p> <p>Nicotinamide adenine dinucleotide (NAD⁺) is an important multifunctional small molecule involved in energy metabolism and modification of DNA/proteins in order to integrate cellular homeostasis and survival. Interestingly, tissues from aged mice have been found to be depleted of intracellular NAD⁺ level partly due to the decrease of Nicotinamide phosphoribosyl-transferase (NAMPT), a rate-limiting enzyme in the NAD⁺ salvage pathway. <i>In vitro</i> NAMPT inhibition in human cells has been shown to deplete NAD⁺ level and promote cellular senescence, while on the contrary, NAMPT upregulation through <i>Nampt</i> cDNA infection can increase NAD⁺ level and promote cellular proliferation. Although this suggests a role for NAMPT in supporting NAD⁺-regulated cellular proliferation and senescence, it is not known if the same effects are conserved in mouse embryonic fibroblast (MEF) cells.</p> <p>Exogenous nicotinamide mononucleotide (NMN; an NAMPT product and precursor to NAD⁺) supplementation was utilized to pharmacologically increase intracellular NAD⁺ level in wild type MEF cells but surprisingly unable to enhance population doubling capacity in MEF cells. Furthermore, MEF cells derived from mice with stable overexpression of <i>Nampt</i> (<i>Nampt</i>-OE) was utilized to investigate the effect of constitutively elevated intracellular NAD⁺ level on cellular proliferation. <i>Nampt</i> overexpression managed to elevate intracellular NAD⁺ level and enhanced the population doubling capacity compared to wild type (WT) MEF cells. Senescence markers such as <i>p21^{CIP}</i>, <i>p19^{ARF}</i> and <i>p16^{INK4a}</i> expressions as well as senescence-associated β-galactosidase (SA-β-gal) activity were reduced, indicating an impact on the onset of senescence by NAD⁺ upregulation in <i>Nampt</i>-OE cells.</p> <p>As <i>in vitro</i> culture primary cells under atmospheric oxygen condition has been associated with replicative senescence, it is hypothesized that the delayed onset of senescence by increased NAD⁺ observed in <i>Nampt</i>-OE cells is mediated by enhanced mitigation of oxidative stress. Measurement of reactive oxygen species (ROS) level revealed that <i>Nampt</i>-OE cells indeed have lower intracellular ROS level compared to WT cells, suggesting an increase in ROS scavenge activity and increased resistance towards oxidative stress. Indeed, <i>Nampt</i>-OE cells also showed improved cell viability and replicative potential, under acute and chronic oxidative stress challenge, respectively. Furthermore, <i>Nampt</i>-OE cells were found to have increased <i>SOD2</i> and <i>Catalase</i> (ROS scavenging enzymes) gene expression. SIRT1 is a NAD⁺-dependent enzyme and is known to</p>			

regulate *SOD2* and *Catalase* (ROS scavenging enzymes) gene expressions by the activation of the transcription factor FOXO1. Consistent with these notions, SIRT1 activity was found to be increased in *Nampt*-OE cells consistent with high level of NAD⁺ in *Nampt*-OE cells.

In conclusion, this study suggests that increasing intracellular NAD⁺ level by overexpressing *Nampt* can influence cell proliferation/senescence fate in murine cells, similar to that observed in the human cells. This is achieved by increasing NAD⁺ in turn enhance SIRT1-mediated antioxidant activity and bolster the resistance against oxidative stress. These findings are hoped to have an implication on senescence and aging researches in particular drug discovery manipulating NAD⁺ synthetic pathways.

List of content

Abstract	2
List of content	4
List of figures	7
Abbreviations	8
1.0 Introduction	10
1.1 Cellular senescence	10
1.2 Replicative senescence	11
1.3 NAD ⁺ and NAMPT modulation regulate cellular senescence	13
1.4 NAD ⁺ biosynthesis	14
1.5 Objective	15
2.0 Materials and methods	17
2.1 Reagents and antibodies	17
2.2 Animals	17
2.3 Cell culture and maintenance	17
2.3.1 MEF isolation for primary cell cultivation	17
2.3.2 Cell culture	18
2.3.3 Cell proliferation assay	18
2.4 NAD ⁺ measurement	19
2.5 Gene expression quantification using real-time PCR	19
2.5.1 RNA extraction	19
2.5.2 cDNA synthesis	20

2.5.3 Real-time quantitative PCR (qPCR)	20
2.6 Protein analysis	21
2.6.1 Protein extraction	21
2.6.2 Protein quantification	22
2.6.3 Western blotting	22
2.6.3.1 Immunoprecipitation	22
2.6.3.2 SDS-PAGE and membrane blotting	22
2.7 MTT (3-(4,5-dimethylthiazol-2-yl)-2,5-diphenyltetrazolium bromide) assay	23
2.8 ATP (Adenosine triphosphate) assay	24
2.9 Senescence-associated β -galactosidase (Sa β -Gal) assay	24
2.10 Cell viability test	25
2.11 ROS measurement assay	25
2.12 SIRT1 activity	25
2.13 Statistical analysis	26
3.0 Results	27
3.1 NAD ⁺ and NAMPT levels decrease in higher cell passage number MEF cells	27
3.2 Supplementation of NMN did not improve cellular proliferation and cellular senescence	28
3.3 Generation and evaluation of <i>Nampt</i> -overexpression (<i>Nampt</i> -OE) transgenic line	30
3.4 <i>Nampt</i> -OE transgenic line shows delayed cellular senescence	33
3.5 <i>Nampt</i> -OE cells exhibit enhanced ROS mitigation and higher cell proliferation potential under oxidative stress condition	38
3.6 <i>Nampt</i> -OE cells exhibit increased ROS scavenging activity	40

3.7 <i>Nampt</i> -OE cells show increased SIRT1 deacetylase activity	42
4.0 Discussion	43
4.1 NAD ⁺ level decreased in passaged MEF cells	43
4.2 Supplementation of NMN did not improve cellular proliferation and cellular senescence	44
4.3 NAMPT overexpression boosts mitochondrial functions	45
4.4 NAMPT overexpressing cells show higher proliferation doubling capacity due to improved oxidative stress mitigation	46
5.0 Concluding remarks	49
6.0 Acknowledgement	51
7.0 References	52

List of figures

Figure 1	p53-pRB mediated pathway to senescence	12
Figure 2	NAD ⁺ biosynthesis pathway in mammalian cells	15
Figure 3	NAD ⁺ and NAMPT protein levels decreased in passaged MEF cells	27
Figure 4	NMN treatment did not affect cellular proliferation and senescence	29
Figure 5	A schematic representation of the expression vector construct carrying human <i>Nampt</i> gene	30
Figure 6	Variable level of NAMPT overexpression and NAD ⁺ in MEF cells isolated from <i>Nampt</i> -OE transgenic mice	32
Figure 7	Changes in mitochondrial properties in MEF cells isolated from <i>Nampt</i> -OE transgenic mice	33
Figure 8	Changes in cell proliferation in MEF cells isolated from <i>Nampt</i> -OE transgenic mice	35
Figure 9	<i>Nampt</i> -OE MEF cells have lower presence of senescent cells	36
Figure 10	<i>Nampt</i> -OE MEF cells have low p16 ^{INK4} , p19 ^{ARF} , p21 ^{CIP1} expression	37
Figure 11	<i>Nampt</i> -OE MEF cells have higher viability level under acute H ₂ O ₂ -induced oxidative stress condition	39
Figure 12	<i>Nampt</i> -OE MEF cells have higher proliferative potential under chronic H ₂ O ₂ -induced oxidative stress condition	40
Figure 13	<i>Nampt</i> -OE MEF cells have lower ROS level than wild type MEF cells	41
Figure 14	<i>Nampt</i> -OE MEF cells have upregulated <i>Sod2</i> and <i>Catalase</i> gene expression	41
Figure 15	SIRT1 activity is increased in <i>Nampt</i> -OE MEF cells	42

Abbreviations:

ATM	Ataxia telangiectasia mutated
ATR	Ataxia telangiectasia mutated and RAD3-related
BamH1	<i>Bacillus amyloliquefaciens</i> H1
Bmal1	Brain and muscle Arnt-like protein-1
C57BL/6	C57 black 6
Cat	Catalase
CD38	cluster of differentiation 38
Cdk2	Cyclin-dependent kinases 2
Cdk4,6	Cyclin-dependent kinases 4,6
Chk1/Chk2	Checkpoint kinase 1/2
CycD	cyclin D
CycE	cyclin E
DMEM	Dulbecco's Modified Eagle Medium
dNTPs	deoxynucleotides
DTT	Dithiothreitol
E2F	E2 factor
Ets1,2	E-twenty-six 1,2
FOXO	Forkhead box O
gamma-H2AX	gamma H2A histone family, member X
Gpx1	Glutathione peroxidase 1
HRP	Horseradish peroxidase
MDM2	Mouse double minute 2 homolog
NNMT	Nicotinamide N-Methyltransferase
p16 ^{INK4a}	p16 Inhibitor of cyclin-dependent kinase type 4
p19 ^{ARF}	p19 Alternate open Reading Frame
p21 ^{CIP1}	p21 CDK-interacting protein 1
PAGE	polyacrylamide gel electrophoresis
PARP	Poly (Adenosine diphosphate ribose) polymerase
PBS	Phosphate buffer saline
pCMV	Cytomegalovirus plasmid

pRb	Retinoblastoma protein
PVDF	polyvinylidene difluoride
<i>Pvu1</i>	<i>Proteus vulgaris</i> 1
RIPA	Radioimmunoprecipitation assay buffer
SDS	sodium dodecyl sulfate
Sod1	Superoxide dismutase 1
Sod2	Superoxide dismutase 2
TRF2	Telomeric repeat-binding factor 2
VDAC	Voltage-dependent anion channels

1.0 Introduction

1.1 Cellular senescence

Cellular senescence is a condition that describes the state of cells that had lose the ability to proliferate in response to various stressors. This non-proliferating state is irreversible even under the stimulation of mitotic signals and is accompanied by changes in morphology as well as metabolic patterns. Among the common attributes of cellular senescence are enhanced lysosomal β -galactosidase activity (Lee *et al.*, 2006), cell cycle arrest at both G1 and G2 phases of the cell cycle (Mao *et al.*, 2012; Johmura *et al.*, 2014), increased level of phosphorylated gamma-H2AX (marker of DNA double strand break) (Sedelnikova *et al.*, 2004), increased level of histone H3K9 methylation in senescence-associated heterochromatin foci (SAHF; Narita *et al.*, 2003), increased stabilization of tumor suppressor protein p53 and p19 as well as elevated levels of cyclin-dependent kinase (CDK) inhibitors p16, p21 (Klement & Goodarzi, 2014), and quite recently, increased secretory behavior termed senescence-associated secretory phenotype (SASP; Coppe *et al.*, 2008; Kulman & Peepers, 2009).

Cellular senescence is a tightly regulated process and is a double-edged sword in terms of its effects on tissue microenvironment. It is beneficial for embryonic development, tissue repair and wound healing, usually under acute senescence response and rapid clearance by the immune system. However, chronic senescence can lead to unwarranted growth, extensive microenvironment remodeling and chronic inflammation that can deplete the affected tissues of replication-competent cells to support homeostasis, as well as increasing the risk of tumorigenesis and drive tissue degeneration and dysfunction that is common in age-related pathogenesis. In fact, senescent cells were shown to underlie age-related diseases across different organs such as brain, eye, muscle, liver, bone and colon (Naylor *et al.*, 2013). Accordingly, removal of senescent cell *in vivo* through targeted elimination (Baker *et al.*, 2011; 2016) or by senolytic drugs (Chang *et al.*, 2016; Yosef *et al.*, 2016) is able to delay tissue degeneration, rejuvenate tissue functions, improve healthy aging process and extend lifespan in mice. These findings demonstrate that cellular senescence is closely linked to age-related pathogenesis and aging.

1.2 Replicative senescence

Replicative senescence (RS) is one type of cellular senescence. RS is induced when telomeres reach their critical length and become incapable to form the A-T loop structure to protect chromosome ends. Exposed chromosome ends could instigate a DNA damage response (DDR) that would activate senescence (Shawi & Autexier, 2008).

RS is differently regulated between species. This is due to the ability of some species to maintain telomerase expression in somatic cells throughout their lives. Telomerases are ribonucleoprotein reverse transcriptase that resynthesize chromosome ends that was lost after every DNA replication. In mammals, its expression is often restricted to the embryogenesis stage (Bekaert *et al.*, 2004), leading to the gradual loss of telomeres in somatic cells. Among those organisms are ungulates (cows, sheeps, horses) and primates (chimpanzees, orangutans, macaques) and humans (Gorbunova & Seluanov, 2009). Telomerase activity however has been reported in the fibroblast of small-sized mammals such as house mouse, naked mole rats, deer mouse, chipmunks and squirrels (Gorbunova & Seluanov, 2009). This allows the cells from these animals to maintains telomere length and escape the onset of replicative senescence. Other examples of organisms with somatic telomerase activity are zebrafish (Tsai *et al.*, 2007) and seabirds (Hausmann *et al.*, 2007).

Under culture condition, human, mouse and chicken fibroblast cells exhibit different proliferation and senescent behavior. It is typical for mouse embryonic fibroblast (MEF) cells that are maintained *in vitro* to have distinctly short proliferation doubling capability, normally around 10-15 times before turning senescent. This doubling rate is considered low when compared to human and chicken fibroblast cells that can maintain proliferation doubling capability up to 50-60 times and 30-40 times *in vitro*, respectively. This is despite the fact that murine cells have longer telomeres (25~150kb) than human and chicken cells (15~20kb; Shay & Wright, 2000; Venkatesan *et al.*, 1998).

Cell culture condition at ~20% atmospheric oxygen pressure causes 20-fold increase in oxygen tension on MEF cells (1.5-3.5% *in vivo* oxygen pressure; Kurosawa *et al.*, 2006; Fischer & Bavister, 1993). This condition has thus been identified to cause an increase in oxidative stress-associated mutation frequency in MEF cells that promotes conversion to senescence. In line with this, MEF cells maintained at 3% oxygen level culture condition did not exhibit senescent characteristics (Busuttil *et al.*, 2003; Parrinello

et al., 2003). Therefore, oxidative stress is regarded as a major cause of MEF cells senescence *in vitro* in contrast to human fibroblast cells that normally turn senescent due to telomere-induced stresses (Parrinello *et al.*, 2003). Similarly, lack of telomere repeat sequence, instead of telomere shortening, causes telomere length deregulation and p53 activation in chicken fibroblast cells (Kim *et al.*, 2002).

Because the prominent activator of senescence differs in human and mouse during culture, the way these cells engage the senescence mechanism also differs. In human cells, telomere-mediated senescence usually engages the ATM-p53-p21^{CIP1} pathway to activate pRb-mediated cell cycle arrest, with p16^{INK4a}-pRb pathway's influence on senescence was shown to be cell type-dependent. Inactivation of both p53 and pRb have caused cells to bypass senescence induced by TRF2 deactivation (Smogorzewska & de Lange 2002). In mouse cells, senescence activation relies primarily on p53 stabilization by p19^{ARF}-MDM interaction. Most MEF cells that overcome senescence displayed loss of p53 function (Harvey & Levine, 1991). p19^{ARF} also have been shown to be upregulated in senescent MEF cells and p19^{ARF} mutant MEF cells does not senesce (Kamijo *et al.*, 1997; Zindy *et al.*, 1998). p21^{CIP1} and p16^{INK4a} are also induced but not essential to establish senescence (Figure 1).

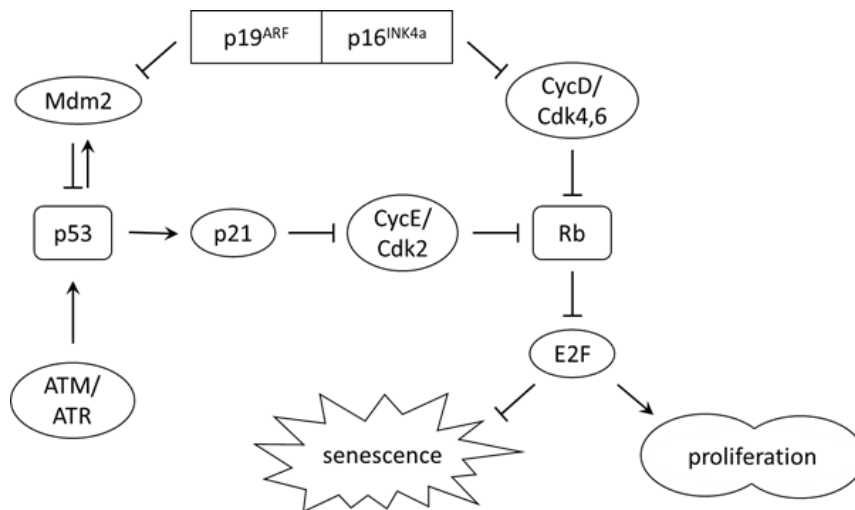


Figure 1: p53-pRb mediated pathway to senescence (modified from Ben-Porath & Weinberg, 2004).

1.3 NAD⁺ and NAMPT modulation regulate cellular senescence

In recent years, NAD⁺ have been gaining attention as an important effector for cellular senescence. NAD⁺ is a form of activated carrier molecule for cellular metabolism that is involved in glycolysis, β -oxidation and oxidative phosphorylation pathways. NAD⁺ also is a co-enzyme for NAD⁺-dependent enzymes important for cellular processes such as energy metabolism and homeostasis, cell death, aging, mitochondrial function, calcium homeostasis and inflammation.

It has been reported that in aging human tissues, there is an increase in activity of NAD⁺-consuming enzymes that regulate cellular homeostasis, DNA repair, cell death and inflammation which also is accompanied by a decrease in NAD⁺ level (Massudi *et al.*, 2012; Camacho-Pereira *et al.*, 2016). Decline in NAD⁺, NAMPT level and activity (involved in NAD⁺ biosynthesis) was also studied in subcultured primary human smooth muscle cells (SMC) and human aortic endothelial cells (HAEC; van der Veer *et al.*, 2007; Borradaile *et al.*, 2009). Increasing intracellular NAD⁺ level through supplementation of NAD⁺ intermediates, on the other hand, was successful in slowing down senescence of human keratinocytes and human fibroblast cells *in vitro* (Lim *et al.*, 2006; Kang *et al.*, 2006).

Limited observations regarding NAD⁺ and NAMPT effect on cellular senescence in non-human organisms are mostly done in rodents. NAD⁺ level was shown to be on a systemic decline in aging tissues of rats (Braidy *et al.*, 2011) and mice (Mouchiroud *et al.*, 2013; Stein *et al.*, 2014). This condition probably correlates with the decrease in NAMPT level (Koltai *et al.*, 2010; Stein *et al.*, 2014). Furthermore, mice administered with NAD⁺ intermediates through dietary supplementation showed an increase in NAD⁺ level and results in resistance to age-related pathogenesis and improved healthy aging (Liu *et al.*, 2013; Canto *et al.*, 2012; Scheibye-Knudsen *et al.*, 2014). Similar results were observed upon knocking out NAD⁺-consuming enzymes PARP1 or CD38 in mice (Bai *et al.*, 2011; Barbosa *et al.*, 2007). However, the question whether these supplementations have any impact on cellular senescence process in mouse tissues have not been addressed.

Nampt overexpression in tissues also have shown promising results, but information is only related to human cells. *Nampt* overexpression promoted NAD⁺ level and extended replicative lifespan in HAEC and human SMC (Borradaile *et al.*, 2009; van der Veer *et al.*, 2007). Others have reported the effect of *Nampt* overexpression in

increasing NAD⁺ level of the skeletal muscle in mice (Frederick *et al.*, 2015), and enhancing protection against cell death in cardiac muscles (Hsu *et al.*, 2009) and neuronal cells (Wang *et al.*, 2012). However, it is not clear whether *Nampt* overexpression would have similar positive effects on cell proliferation and senescence in mice and remain to be tested. It is noteworthy that the advantageous outcomes of the increase in NAMPT/NAD⁺ axis seen in mice and humans also relied on the increase in SIRT1 regulatory functions, highlighting the potentially close relationship between NAD⁺ and cellular proliferation machinery, cell fate and aging.

1.4 NAD⁺ biosynthesis

NAD⁺ biosynthesis is a highly regulated process that consists of multiple alternative routes to ensure NAD⁺ homeostasis. NAD⁺ biosynthesis in animals mainly follows three different pathways: *de novo* pathway, Preiss-Handler pathway and the salvage pathways (de Figueiredo *et al.*, 2011). *De novo* pathway utilizes amino acid L-tryptophan as the starting material to generate quinolinic acid through multiple enzymatic conversions. Quinolinic acid is further converted to nicotinic acid mononucleotide (NaMN) by the addition of a phosphoribosyl group followed by an addition of an adenylyl group to form nicotinic acid adenine nucleotide (NaAD/deamido-NAD) and finally an amidation of the nicotinic acid moiety to generate NAD⁺. Preiss-Handler pathway shares the same pathway as in *de novo* but uses nicotinic acid (NA) obtained from diet instead to produce NaMN (Figure 2).

On the other hand, NAD⁺ salvage pathway is more simplistic and provides a more rapid alternative to NAD⁺ biosynthesis as opposed to *de novo*. In particular, nicotinamide phosphoribosyl transferase (NAMPT) ‘salvages’ free nicotinamides (catabolized from NAD⁺ by NAD⁺-dependent enzymes) by transferring them to phosphoribosyl phosphates to form nicotinamide mononucleotide (NMN). Subsequently nicotinamide mononucleotide adenylyl transferase (NMNAT) mediates condensation of NMN with ATP to generate NAD⁺. Alternatively, nicotinamide ribose (NR) are utilized to generate NMN and this is carried out by nicotinamide ribose kinase (NRKs; Figure 2).

NAMPT is expressed at a basal level to preserve NAD⁺ homeostasis under constitutive PARP1 activity but its level can be modulated to adapt to NAD⁺ demand during energy and nutritional perturbation such as physical exercise, calorie restriction

and diet variation (Pittelli *et al.*, 2010; Yoshino *et al.*, 2011; Ruggieri *et al.*, 2015). NAMPT enzyme is therefore considered as the rate-limiting enzyme for this pathway, supported by the fact that overexpression of NAMPT, but not NMNAT, was found to increase NAD⁺ level in mouse fibroblast (Revollo *et al.*, 2004).

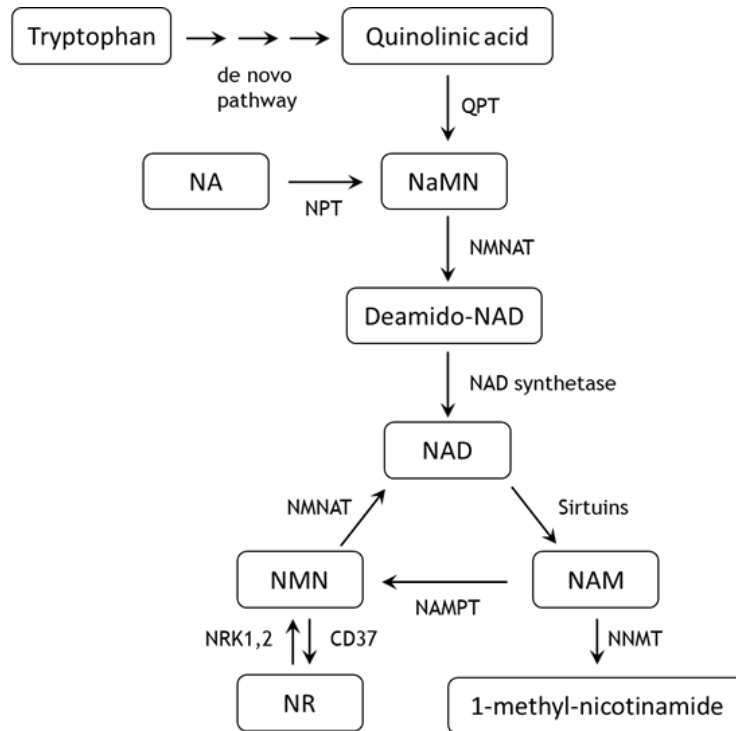


Figure 2: NAD⁺ biosynthesis pathway in mammalian cells (modified from Imai & Guarente, 2014).

1.5 Objective

Studies on cellular senescence and longevity are gaining traction especially with the discovery that intracellular NAD⁺ pool poses as a key factor in fending off senescence onset and degradation associated with aging. Most efforts would rely increasingly on manipulation in murine models to reveal the underlying mechanisms. However, it is becoming evident that mechanism that NAD⁺ levels as well as the mechanism that regulates senescence in mammalian cells varied between species. These variables warrant some thorough considerations if one were to draw mouse-to-human comparisons (Itahana *et al.*, 2004). To bridge this gap in the knowledge of murine cellular senescence, this study attempts to test the effects of pharmacological (NMN supplementation) and genetic manipulations (*Nampt* overexpression) on NAD⁺ homeostasis and on cellular senescence.

This approach also would potentially allow for comparative metabolic and behavioral analysis across multiple tissue types and stress conditions in hope to yield substantial information that can benefit the efforts to understand and promote healthy aging.

2.0 Materials and Methods

2.1 Reagents and Antibodies

Nicotinamide mononucleotide (NMN) was purchased from Sigma-Aldrich. Antibodies against HA (M180-3), NAMPT (D7V5J) and β -Actin (AC-15) were purchased from MBL (Nagoya, Japan), CST and Sigma-Aldrich, respectively. VDAC antibody was purchased from Cell Signaling (#4866). Secondary HRP-conjugated anti-mouse/rabbit IgGs were purchased from GE Healthcare. pCAGGS and h *Nampt*-HA/pCMV vectors were kindly gifted by Drs H. Niwa and I. Shimomura, respectively.

2.2 Animals

C57BL/6 mice purchased from Japan SLC, Inc. (Hamamatsu, Japan) were housed under 12-h light/12-h dark cycles. Human *Nampt* coding sequence with HA tag at 3' region in pCMV was subcloned into pCAGGS vector and digested by *PvuI* and *BamHI* to produce transgenic mice by microinjecting into the pronuclei of fertilized eggs of C57BL/6 mice. We used in this study 4 out of 5 transgenic (Tg) mice, which have transgenes in a single genome region confirmed by southern blotting analyses (data not shown). Tg mice were crossed with C57BL/6 female mice to generate primary mouse embryonic fibroblast (MEF) cells. Our experiments were approved by the Animal Care Committee of Nara Institute of Science and Technology and conducted in accordance with guidelines that were established by the Science Council of Japan.

2.3 Cell culture and maintenance

2.3.1 MEF cell isolation for primary cell cultivation

Preparation of MEF primary cultures was carried out according to procedures described by Jozefczuk *et al.*, (2009). Pregnant wildtype and NAMPT transgenic mice (13-14 days post-coitum) were sacrificed by means of cervical dislocation. Next, the lower part of the abdomen was dissected and the uterine horn was recovered. The uterine horn was rinsed first in 70% ethanol and later 1X PBS. After moving to the biosafety cabinet, the embryos were isolated from the uterus and placed in 1X PBS. Next, the head and red-colored tissue/organs were carefully removed from each embryo and the

remaining parts were minced finely using surgical blades. After that, 2ml trypsin (0.53mmol/L) was added to the minced tissues and incubated at 37°C for 10 mins. Then, the minced tissues were resuspended in trypsin by pipetting and transferred to conical tubes containing 8ml MEF culture media (DMEM High Glucose (Nacalai) supplemented with 1mM sodium pyruvate (Nacalai), 1X non-essential amino acids, 100µM β-mercaptoethanol (Gibco), 10% FBS (Biowest), (1%) penicillin streptomycin (Nacalai), 100µg/ml primocin (InvivoGen)). The samples were left to stand for 5 mins. Finally, the media was aspirated and transferred onto 10cm culture dishes. At this stage, cells are designated as cells at passage 1. The cells were incubated at 37°C, 5% CO₂ overnight. The next day, cells were subcultured or cryopreserved in CellBanker (Nippon Zenyaku Kogyo) solution and kept in -80°C for long term storage.

2.3.2 Cell culture

10cm dish vessel containing cells at 70-90% confluency were trypsinized for 5 mins at 37°C. Then, 10ml MEF culture media was added to the cells to deactivate the trypsin. Cell suspension was then transferred into a conical tube and centrifuged at 1000rpm for 5 mins. The supernatant was discarded and cell pellet was resuspended in 1~5ml MEF media. 10µl cell suspension was mixed with trypan blue dye and used for cell counting using haemocytometer. Appropriate volume of cell suspension equivalent to 5x10⁵ cells were seeded in 10ml MEF media on a new 10cm dish. The cells were then incubated at 37°C, 5% CO₂.

2.3.3 Cell proliferation assay

Cells at passage 2 were cultured in 6-well plate at seeding density of 1x10⁵ per well with or without the presence of NMN. The cells were then maintained at 37°C, 5% CO₂ and subcultured for every three days with growth media freshly supplemented with NMN. Cell count was done before each subculture and population doubling level (PDL) was calculated using the following formula: $3.32(\log[\text{total viable cells at harvest}/\text{total viable cells at seeding}])$. The life span of the cells was presented as cell growth curve of cumulative PDLs versus time in culture.

2.4 NAD⁺ measurement

To measure intracellular NAD⁺, NAD/NADH-GloTM Assay (Promega) was used. Cells were seeded in 96-well plates. After culturing for 24 hours, cells were washed with PBS and were resuspended well in 50µl 1X PBS and 50µl 0.2N NaOH supplemented with 1% dodecyl trimethyl ammonium bromide (DTAB). The cell suspension was mixed by repeated pipetting to lyse the cells. Next, 50µl of the cell lysate was transferred to a new 1.5ml Eppendorf tube followed by adding 25µl 0.4N HCl. The tube was flicked to mix the content and then incubated at 60°C for 15 mins. Then it was left to stand at RT to cool down for 10 min. Later, 25µl of 0.5M Trizma base solution was added to the mixture and transferred to a 96-well microplate.

To detect luminescence signals, NAD/NADH-Glo Detection Reagent was added to an equal volume to the sample and incubated 30 min, then signal was measured using a microplate reader (Mithras).

2.5 Gene expression quantification using real-time PCR

2.5.1 RNA extraction

Cells grown in culture dishes to 70-90% confluency were washed with 1X PBS and then trypsinized using Trypsin for 5 mins at 37°C. Culture dish were tapped lightly several times to facilitate cell dissociation and MEF media was added to the cells to stop the reaction. Depending on the volume, detached cells were either transferred into conical or 1.5ml Eppendorf tubes and centrifuged at 1000rpm for 5 mins at room temperature to pellet the cells. Supernatant fraction was discarded and followed by resuspending the cells in 1ml Sepasol RNA 1 Super G (Nacalai). Cells were mixed by flicking the tubes and left to stand at RT for 5 mins before 200µl chloroform is added to each tube. The content was mixed by inverting the tubes several times and left to stand at RT for 10 mins.

Afterwards, the mixture was centrifuged at 12,000xg for 15 mins at 4°C to obtain the aqueous phase that contains the RNA fractions. 500-600µl of the aqueous phase was transferred to new 1.5ml Eppendorf tubes and further added with equal volume of isopropanol. The mixture was again mixed by tube inversion and left to stand at room temperature for 10 mins. Next, the mixture was centrifuged at 12,000xg for 10 mins at 4°C to pellet the RNA. Supernatant was discarded and RNA pellet was rinsed by adding 75% ethanol and followed by centrifugation at 12,000xg for 5 mins at 4°C. The

supernatant was discarded carefully without disturbing the RNA pellet. RNA pellet was air-dried for 10 mins at room temperature before it was dissolved in purified water. RNA pellet was heated on a heat block to 60°C for 10 mins and allowed to cool down in ice afterwards. RNA quantitation was carried out using Nanodrop spectrophotometer (Thermo Scientific). Purified RNA samples are kept at -80°C for long term storage.

2.5.2 cDNA synthesis

1µg of total RNA was converted to complementary DNA (cDNA) by reverse-transcription PCR using SuperscriptTM II Reverse Transcriptase (Invitrogen) according to the manufacturer's protocol. Each reaction consists of 1µg RNA extract, 1X First-Strand Buffer, 10mM DTT, 1mM dNTPs, 250ng random primers and topped up with purified autoclaved water to a final volume of 20µl. First, RNA samples were added to random primers, dNTPs and water in a PCR strip and were heated to 65°C for 10 mins. Then, First-Strand Buffer, 10mM DTT, and Reverse Transcriptase were added to each sample. The samples were then heated up to 42°C for 2 hours followed by 70°C for 15 mins. The cDNA products are kept in -20°C freezer for long term storage.

2.5.3 Real-time quantitative PCR (qPCR)

qPCR was carried out using SYBR Green dye from KAPA SYBR FAST qPCR kit mastermix (KAPA BIOSYSTEMS) following the manufacturer's protocol. Each reaction consists of 1X KAPA SYBR FAST qPCR Master Mix universal, 200nM of forward and reverse primers, 20ng of cDNA products and topped water to a final volume of 10µl. All reagents except the cDNAs were prepared in a mastermix and aliquoted into wells of a white multiwell plate before lastly adding the cDNA samples. qPCR was carried out using Lightcycler 480 instruments and the result was analysed using LightCycler 480 Software Version 1.5 (Roche). Samples were heated to 95°C for initial denaturation followed by 40 sets of denaturation at 95°C for 10 secs, hybridization at 60°C for 20 secs followed by elongation at 72°C for 1 sec. Fold change of target gene transcripts was measured using absolute quantification method and normalized to 18s rRNA gene expression as endogenous control. The sequences of the forward and reverse primers for mice were as follows:

Nampt Fw: TGGCCATGATCTTCTCCATACG
Nampt Rv: ACATAACAACCCGGCCACAT
18S rRNA Fw: CGCCGCTAGAGGTGAAATTC
18S rRNA Rv: CGAACCTCCGACTTTCGTTCT
p16^{INK4a} Fw: CGAACTCTTTCGGTCGTACCC
p16^{INK4a} Rv: CGAATCTGCACCGTAGTTGAGC
p19^{ARF} Fw: GTTCTTGGTCACTGTGAGGATTCAG
p19^{ARF} Rv: CCATCATCATCACCTGGTCCAG
p21^{CIP1} Fw: GCAGATCCACAGCGATATCCAG
p21^{CIP1} Rv: CGAAGAGACAAGGGCACACTTT
sod1 Fw: GAGACCTGGGCAATGTGACT
sod1 Rv: GTTTACTGCGCAATCCCAAT
sod2 Fw: GGAGCAAGGTCGCTTACAGA
sod2 Rv: GTGCTCCCACACGTCAATC
catalase Fw: AAATGCTTCAGGGCCGCCTT
catalase Rv: GTAGGGACAGTTCACAGGTA
gpx1 Fw: AGTTCGGACACCAGGAGAAT
gpx1 Rv: GAAGGTAAAGAGCGGGTGAG

2.6 Protein analysis

2.6.1 Protein extraction

Cells grown in culture dishes to 70-90% confluency were washed with 1X PBS and then trypsinized using Trypsin for 5 mins at 37°C. These culture dishes were tapped lightly several times to facilitate cell dissociation and MEF media was added to the cells to stop the reaction. Depending on the volume, detached cells were either transferred into conical or 1.5ml Eppendorf tubes and centrifuged at 1000rpm for 5 mins at room temperature to pellet the cells. Supernatant fraction was discarded and followed by resuspending the cells in 1ml of RIPA buffer containing 1X proteinase inhibitor cocktail (Nacalai). Cells were mixed by flicking the tubes and incubated on ice for 10 mins. The mixture was then vortexed vigorously for 10 secs and incubated on ice for another 10 mins. Later, the mixture was centrifuged at 15,000rpm for 15 mins at 4°C to pellet the

cell debris. The supernatant containing total proteins was then transferred to new 1.5ml Eppendorf tubes. Purified protein samples are kept at -80°C for long term storage.

2.6.2 Protein quantitation

Total protein concentration was measured using PIERCE 660nm Protein Assay reagent (Thermo Scientific) according to the manufacturer's protocol. Protein samples were mixed with Protein Assay reagent at 1:15 ratio in 1.5ml Eppendorf tubes and vortexed briefly to mix. Samples were then covered and left to stand at room temperature for 5 mins before being transferred to disposable cuvettes. Measurements were carried out at 660nm wavelength and normalized to control reaction containing water or RIPA buffer.

2.6.3 Western blotting:

2.6.3.1 Immunoprecipitation

Protein samples were first diluted in RIPA buffer to a final concentration of 1mg/ml. Then 1µl of primary antibody was added to 1ml of samples and incubated overnight at 4°C on a tube rotator. Next, agarose beads coated with IgG Protein A (Nacalai) that have been rinsed in RIPA buffer beforehand was added to the samples and incubated at 4°C for 3 hours on a tube rotator. Afterwards, the samples were centrifuged at 3000rpm at 4°C for 10 secs to pellet the beads. The supernatant was later removed and the beads were rinsed three times in 1ml RIPA using the same protocol. After the final rinse, the supernatant was removed completely and added with 20µl of 2X denaturing buffer (100mM Tris-HCl (pH 8.6), 4% (w/v) sodium dodecyl sulfate, 0.2% (w/v) bromophenol blue, 20% (v/v) glycerol, 200mM dithiothreitol). The samples were then heated up to 95°C for 5 mins and immediately placed on ice for at least 5 mins to bring the temperature down. Subsequently, the samples were analysed using SDS-PAGE and western blotting as described.

2.6.3.2 SDS-PAGE and membrane blotting

Protein samples were diluted in RIPA buffer to a final concentration of 1mg/ml and added with 4X denaturing buffer (200mM Tris-HCl (pH 8.6), 8% (w/v) sodium dodecyl sulfate, 0.4% (w/v) bromophenol blue, 40% (v/v) glycerol, 400mM

dithiothreitol) containing 1X proteinase inhibitor cocktail (Nacalai). Samples were vortexed briefly to mix, denatured by heating at 95°C for 5 mins and immediately placed on ice for at least 5 mins to bring the temperature down.

SDS-PAGE instruments and precast 5-20% polyacrylamide gels (Nacalai) were set up according to manufacturer's protocol. Each well was flushed with SDS running buffer before 20µg protein samples were loaded into each well. 5µl of Precision Plus Protein™ standard (Bio-Rad) was included in every run to serve as indicator of protein size in kDalton. Samples were electrophoresed at 300V 20mA until the dye front have moved sufficiently down the gel (roughly 60-70 mins).

Resolved proteins were transferred onto Amersham Hybond PVDF membrane (GE Healthcare) using semi-dry transfer set up. Transfer stack was prepared by sandwiching the acrylamide gel and pre-wet PVDF membrane between pre-wet filter papers (both soaked in transfer buffer prior to transfer). Transfer was carried out at 300V 100mA for 60 mins. Upon completion, the membrane was blocked in blocking buffer (5% skimmed milk in 1X TBS-T) for 60 mins with agitation at room temperature. Later, the membrane was rinsed in wash buffer (1X TBS-T) for 10 mins with agitation at room temperature for three times. Membrane was then incubated with agitation in diluted primary antibody for either 60 mins at room temperature or overnight at 4°C. Upon completion, membrane was rinsed in wash buffer as described earlier followed by an incubation with conjugating second antibody (diluted in blocking buffer (5% skimmed milk in 1X TBS-T) with agitation for 60 mins at room temperature. After that, membrane was rinsed in wash buffer as described earlier before being treated with Chemi-Lumi One chemiluminescent reagent (Nacalai) for 5 mins at room temperature. Subsequently, blot imaging was carried out using an X-ray film (Fujifilm) while analysis of band intensity was done using ImageJ software.

2.7 MTT (3-(4,5-dimethylthiazol-2-yl)-2,5-diphenyltetrazolium bromide) assay

MTT Cell Count Kit (Nacalai) was used to measure the mitochondrial condition in the cells based on its dehydrogenase activity. 4000 cells in 100µl were seeded into 96-well plates. Cells were incubated at 37°C, 5% CO₂ for 24 hours before the start of assay. Following that, 10µl of MTT solution (5mg/ml MTT in phosphate buffered saline) was added to each well and the plate was incubated at 37°C, 5% CO₂ for 2 hours. Later, 100µl

of solubilization solution (0.04mol/l HCl in isopropanol) was added to each well and the solution was pipetted repeatedly to dissolve the precipitated formazan. The plate was observed under microscope to ensure that all formazan has dissolved before the absorbance was measured microplate reader (Mithras) at 570nm wavelength.

2.8 ATP (Adenosine triphosphate) assay

To measure the ATP level, the CellTiter-Glo® Luminescent Cell Viability Assay (Promega) was used. 4000 cells in 100µl were seeded into 96-well plates. Cells were incubated at 37°C, 5% CO₂ for 24 hours before the start of assay. H₂O₂ treatment was carried out by adding 100µM H₂O₂ to the cells during seeding. The CellTiter-Glo® Reagent was prepared prior to use by first CellTiter-Glo® Buffer and lyophilized CellTiter-Glo® Substrate were thawed to RT. Then 10ml of CellTiter-Glo® Buffer were added to the lyophilized CellTiter-Glo® Substrate and swirled gently to reconstitute the powder. After cell incubation time is up, equal volume of CellTiter-Glo® (i.e. 100µl) was added to each well. Plate content was then mixed on an orbital shaker for two mins and then left to stand at RT for 10 mins to stabilize the luminescent signal. Signal was then measured using a microplate reader (Mithras).

2.9 Senescence-associated β-galactosidase (Saβ-Gal) assay

Saβ-Gal staining was carried out according to protocol described by Debacq-Chainiaux *et al.* (2009). Cells were subcultured in 35mm culture dish at 1x10⁵ seeding density and incubated at 37°C for 24 hours. Then, the cells were rinsed with 1X PBS twice to remove residual growth media. The cells were then incubated in fix solution (2% formaldehyde and 0.2% glutaraldehyde in water) for 5 mins at room temperature with agitation. After that, the cells were rinsed again with 1X PBS twice before 2ml of Saβ-Gal staining solution (40mM sodium citrate (pH 6.0), 5mM potassium ferrocyanide, 5mM potassium ferricyanide, 1 mg/ml 5-bromo-4-chloro-3-indolyl-β-D-galactopyranoside (X-gal), 150mM sodium chloride, and 2mM magnesium chloride) was added to each dish. Cells were incubated at 37°C without CO₂ for 12-16 hours. Cells were examined under microscope and positively stained cells were counted and photographed.

2.10 Cell viability assay

MEF cells were seeded in 6-well plate at seeding density of 1×10^5 per well and cells were then maintained at 37°C , 5% CO_2 . Then cells were treated with H_2O_2 at the designated concentration for 24 hours. Cell viability was measured using trypan blue staining. Viable cells were counted based on the lack of staining in the cells and normalized to the total number of cells in the viewplane. Calculation was presented in percentage.

2.11 ROS measurement assay

Intracellular ROS level was determined using oxidation probe 5–6-chloromethyl-2',7'-dichlorodihydrofluorescein diacetate (CM-H2DCFDA) kit (Life Technologies). MEF cells were seeded in 6-well plate at seeding density of 1×10^5 per well and cells were then maintained at 37°C , 5% CO_2 . For NMN treatment, 1mM NMN was added to cells 24 hours prior to adding CM-H2DCFDA probe. In the case of H_2O_2 treatment, 100 μM H_2O_2 was added to the culture medium 2 hours before adding CM-H2DCFDA probe. CM-H2DCFDA probe that has been freshly diluted in DMSO was later added to the cells at a final concentration of 10 μM /well. Cells were incubated for 30 mins at 37°C , 5% CO_2 and, trypsinized and counted. 6×10^4 cells were aliquoted into new 1.5ml Eppendorf tubes, and centrifuged to pellet cells. Supernatant was discarded and cell pellets were resuspended in 100 μl 1X PBS and transferred to 96-well microplate. Fluorescence signal were measured using a microplate reader (Mithras) at wavelengths 492–495nm excitation and 517–527nm emission.

2.12 SIRT1 activity assay

Measurement of SIRT1 activity was done using Fluor De Lys SIRT1 Fluorometric activity assay/Drug Discovery Kit (Enzo) according to the manufacturer's guidelines. MEF cells were seeded in 6-well plate at seeding density of 1×10^5 per well and maintained at 37°C , 5% CO_2 . The cells were cultured for 24 hours before 1mM NMN was added to the culture media. The cells were then maintained at 37°C , 5% CO_2 for another 24 hours before cells were trypsinized and counted as described earlier. An appropriate volume of 1×10^5 cells was aliquoted from the cells suspension and centrifuged to pellet the cells. Cells were resuspended well in 50 μl Assay Buffer supplemented in the kit. The cell

suspension was mixed by repeated pipetting and sonicated to lyse the cells. After centrifugation, supernatants, 1U SIRT1 and 0.1mM Substrate were applied to SIRT1 assay to a total reaction volume of 50 μ l.

2.13 Statistical analysis

Values are reported as mean \pm SE. Statistical differences were determined by a Student's t test. Statistical significance is displayed as * ($p < 0.05$) or ** ($p < 0.01$).

3.0 Results

3.1 NAD⁺ and NAMPT levels decrease in higher cell passage number MEF cells

NAD⁺ level has been shown to decline with age in mouse and human tissue biopsies as well as in cultured human cells. However, whether the NAD⁺ level also decrease in primary MEF cells is not known. To address this, we first measured NAD⁺ level in wild type MEF cells and discovered that NAD⁺ level in MEF cells also show a decline with subsequent passages (Figure 3A). We further investigated whether NAMPT level was also affected. As expected, expression level of *Nampt* gene and protein level also showed a decline with passage number progression (Figure 3B, C). These results are consistent with the NAD⁺ decline observed in human cells (van der Veer *et al.*, 2007).

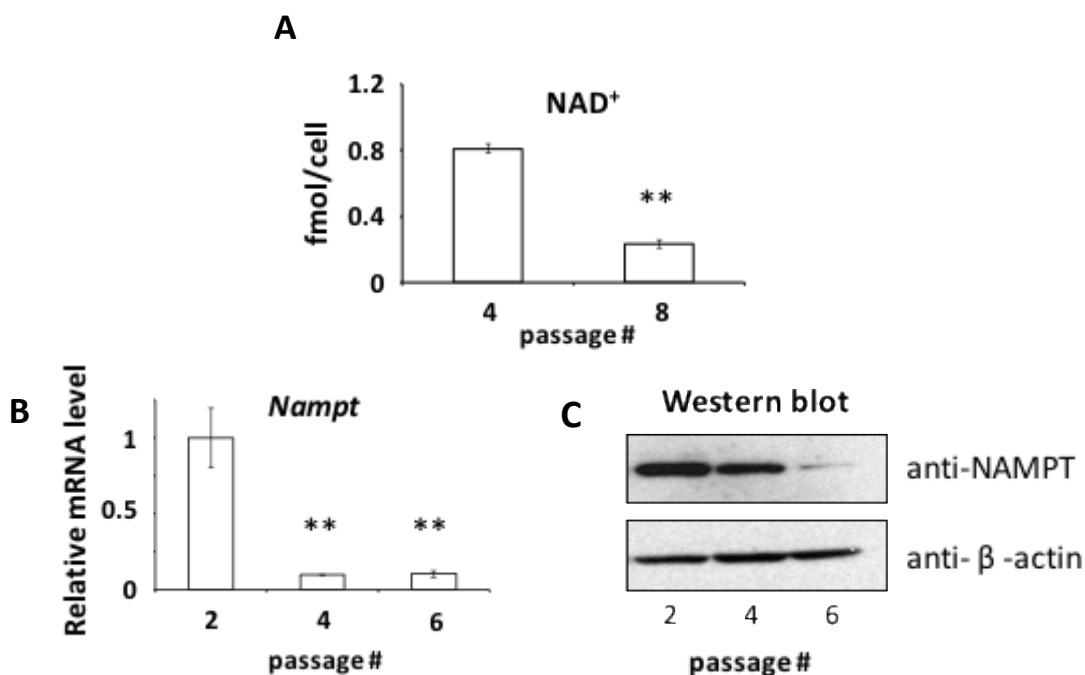


Figure 3: NAD⁺ and NAMPT protein levels decreased in passaged MEF cells. (A) Primary MEFs were isolated and cultured before cell lysate were extracted at passage 4 and 8 before NAD⁺ level were measured using NAD/NADH colorimetric quantification kit. (B) Primary MEFs were isolated and cultured before total RNA was extracted from cells at passage 2, 4 and 6 and subjected to quantitative PCR analysis. Expression level was normalized to *18s rRNA* gene expression. (C) NAMPT protein were isolated from primary MEFs at passage 2,4 and 6 and subjected to western blot analysis. **: $p < 0.01$

3.2 Supplementation of NMN did not improve cellular proliferation and cellular senescence

Increase in cellular NAD⁺ level have been previously linked to improvement in cell proliferation and delay of cellular senescence. The exogenous precursor supplementation approach, in particular, have been shown to be an efficient method to elevate cellular NAD⁺ level and SIRT1 activity (Ho *et al.*, 2009; Jang *et al.*, 2012). Considering these points, we therefore tried to find out if it is possible to slow down the onset of senescence in wild type MEF cells by increasing intracellular NAD⁺ level through exogenous source.

We carried out cell proliferation assay using wild type MEF cells cultured in growth media supplemented with NMN at the beginning of every cell passage. MEF cells were subcultured every 3 days and their cumulative population doubling level (PDL) was recorded. PDL is a measure of cell proliferation rate from a single passage, while cumulative PDL represent the overall proliferation rate throughout the cell culture duration. Monitoring the PDL of cells will enable us to see the effect of NMN treatment on cell proliferation capacity and identify the point of which cell proliferation ceases. Here, we define a cease of cell proliferation (CCP) as the point at which PDL value dips below 0.5.

Of note, NMN is the direct enzymatic product of NAMPT and has been shown to be able to increase intracellular NAD⁺ level of human foreskin fibroblast cells upon 1mM treatment (Song *et al.*, 2015). Accordingly, 1mM NMN treatment was able to increase cellular NAD⁺ level in wild type MEF cells to about two-fold (Figure 4A). However, NMN treatment did not stimulate any significant increase in cell proliferation rate when compared to untreated wild type cells (Figure 4B, C). Both NMN-treated and untreated wild type cells showed similar growth curves, reaching CCP at passage 5 and having cumulative PDL of 8.

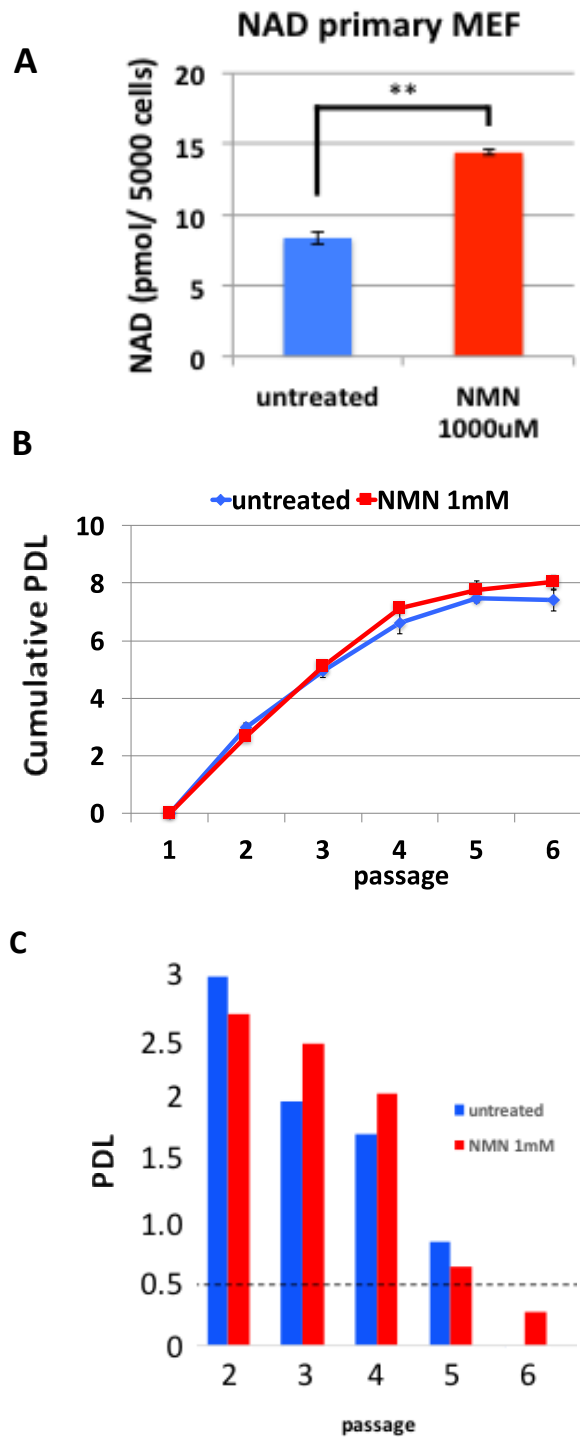


Figure 4: NMN treatment did not affect cellular proliferation and senescence. (A) NAD⁺ measurement of primary wild type MEFs cultured with 1mM NMN for 24 hours. (B) Primary wild type MEFs were cultured with 1mM NMN and cumulative PDL was recorded and analysed to generate a growth curve. (C) PDL level for each passage from the growth curve in (B). Passage with PDL value less than 0.5 threshold (dotted line) is considered to have entered senescence. **: $p < 0.01$.

3.3 Generation and evaluation of *Nampt*-overexpression (*Nampt*-OE) transgenic line

We also took a genetic approach in order to increase cellular NAD⁺. Transgenic mice overexpressing HA-tagged human *Nampt* gene (*Nampt*-OE) under by a CAG promoter (Figure 5) were generated (see section 2.2 of Materials and Methods) and four independent transgenic lines were established (designated as Tg#1, Tg#2, Tg#3 and Tg#4). Immunoblotting against HA or NAMPT proteins from these four lines showed variable magnitude of fold increase in exogenous NAMPT abundance. Line Tg#4 has the highest fold increase (5-fold) followed by line Tg#1, Tg#2 and Tg#3 with 3-fold, 2-fold and 1.5-fold increase, respectively (Figure 6A, B).

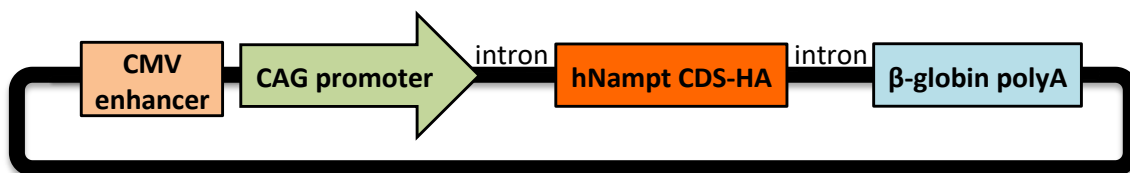


Figure 5: A schematic drawing of the expression vector construct carrying human *Nampt* gene fused with HA tag used in generating *Nampt*-OE transgenic mice.

Considering the fact that NAMPT is the rate-limiting enzyme in the NAD⁺ salvage pathway that is vital for cellular NAD⁺ biosynthesis, we proceeded to measure the total NAD⁺ level under *Nampt* overexpression. As shown in Figure 6C, NAD⁺ level was found to be elevated in a similar pattern to the fold increase of NAMPT abundance in the cells of each transgenic line. At passage 4, cells from line Tg#4 has the highest fold increase (5-fold) followed by line Tg#1, Tg#2 and Tg#3 with 3-fold, 2-fold and 1.5-fold increase, respectively. At passage 8, NAMPT transgenic cells exhibited similar fold increase of NAD⁺ level when compared to wild type cells despite showing an overall decline in NAD⁺ level.

Next, ATP level in *Nampt*-OE cells was measured to see if there is any change to the redox state of the cells due to the increase in NAD⁺ level. Accordingly, ATP level rose in these transgenic cells when compared to wild type cells, with line Tg#4 cells showed the highest fold increase (2.3-fold) followed by line Tg#1, Tg#2 and Tg#3 with 1.6-fold, 1.5-fold and 1.3-fold increase, respectively (Figure 7A). Since ATP production takes place mainly in the mitochondria, we proceeded to check if the mitochondrial redox

activity was upregulated in the transgenic cells. Measurement of mitochondrial activity based on MTT colorimetric assay indicated that mitochondria of *Nampt*-OE cells have higher activity than wildtype cells (Figure 7B). In particular, mitochondria in line Tg#4 cells had 2.6-fold increase in activity, followed by line #1 (2.3-fold) and Tg#2 (2-fold) while Tg#3 showed a slight but statistically insignificant increase.

Comparison of the level of mitochondrial outer membrane protein VDAC by western blotting was also carried out to serve as a readout for any increase in mitochondrial mass. VDAC protein level however was found to be unchanged in all transgenic lines tested when compared to wild type cells, suggesting that *Nampt* overexpression enhanced energy metabolism by increasing mitochondrial redox activity without changing the mitochondrial mass (Figure 7C). Together, these results showed that *Nampt*-OE cells have enhanced NAD⁺ production and that this alteration impacts the cellular energy metabolism.

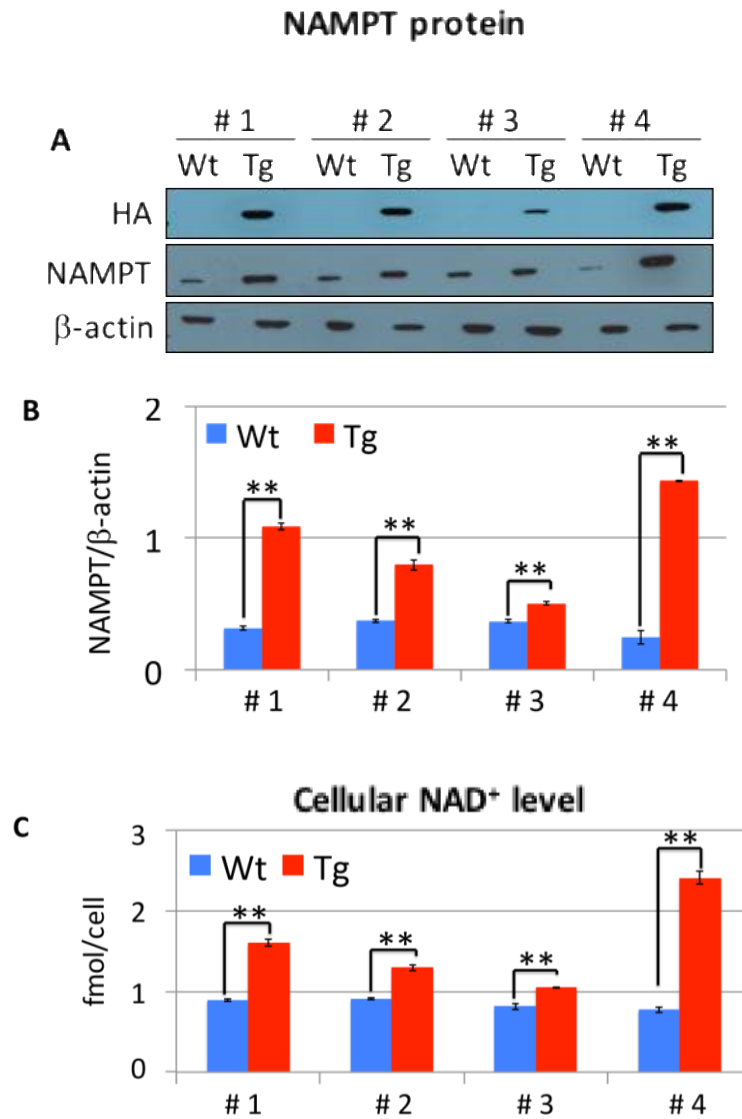


Figure 6: Variable level of NAMPT overexpression and NAD⁺ in MEF cells isolated from *Nampt*-OE transgenic mice. (A) Western blotting analysis against NAMPT and HA. Band intensities of NAMPT were normalized to β -actin and represented in (B). (C) Intracellular NAD⁺ level measured based on recycling NAD⁺ reaction method. **: $p < 0.01$.

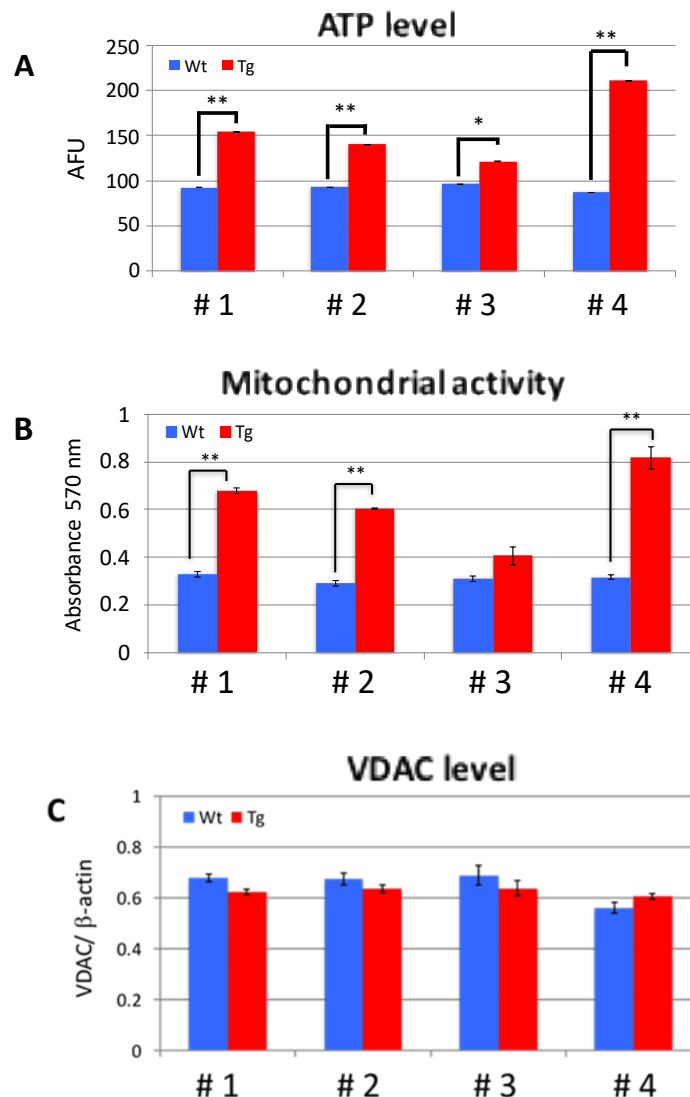


Figure 7: Changes in mitochondrial properties in MEF cells isolated from *Nampt*-OE transgenic mice. (A) Measurement of ATP level using luciferase-based assay. (B) Measurement of mitochondrial activity based on MTT colorimetric assay. (C) Change in mitochondrial mass based on VDAC membrane protein level normalized to β -actin. *: $p < 0.05$; **: $p < 0.01$.

3.4 *Nampt*-OE transgenic line shows delayed cellular senescence

As mentioned before, intracellular NAD^+ level has been causally linked to cellular senescence in human cells. To figure out if *Nampt* overexpression has any effect on cellular proliferation and senescence of MEF cells, we carried out cell proliferation assays. Wild type MEF cells were also obtained from littermates of each transgenic line respectively and cultured in parallel to serve as controls. MEF cells were subcultured every 3 days and their cumulative population doubling level (PDL) was recorded. This

allow us to see the effect of *Nampt* overexpression on cell proliferation capacity and pinpoint when the majority of cells cease to proliferate.

First, we monitored the PDL of the independent wild type MEF cohorts to serve as controls for the *Nampt*-OE MEF cells. PDL analysis revealed that all the wild type MEF cells have similar growth curves, reaching CCP at passage 6 with an average cumulative PDL of 9.52. PDL analysis of *Nampt*-OE cells on the other hand showed mixed results when compared to the wild type cohorts. Line Tg#4 cells reached CCP later than control, at passage 8, with cumulative PDL of 12.8. Line Tg#1 and Tg#2 cells both also reached CCP later than control, at passage 7, with cumulative PDL of 11.9 and 11.7 respectively. Line Tg#3 however reached CCP at passage 6 similar to wild type MEF cells with cumulative PDL of 10. These results suggest that *Nampt*-OE cell had an enhanced proliferation capability than wild type cells and these enhancements correspond to the degree of *Nampt* overexpression and NAD⁺ increase in the respective transgenic MEF cell lines (Figure 8).

We then asked if the enhanced proliferation capability and delayed CCP observed in *Nampt*-OE cells was due to a delay in the onset of cellular senescence. To address this question, we compared the cellular senescence state of wild type and *Nampt*-OE cells by analyzing several senescence markers such as senescence-associated β -galactosidase (Sa β -Gal) activity and quantitative analysis of *p16^{INK4a}*, *p19^{ARF}* and *p21^{CIP1}* gene expression.

Staining for Sa β -Gal activity is a standard method to assess the presence of senescent cells in a cell population based on the reported increased activity of β -galactosidase at suboptimal pH. Sa β -Gal staining of wild type MEF cohort cells revealed that wild type cells started to have dramatic accumulation of Sa β -Gal-positive cells at passage 6, which is consistent with the CCP observed in the PDL analysis. The presence of Sa β -Gal-positive cells continues to increase from 10% to 40% with every subsequent subcultures. On the other hand, *Nampt*-OE MEF cells showed a slow but steady accumulation of Sa β -Gal-positive cells. Unlike their matching wild type cohorts, these *Nampt*-OE MEF cells did not show a dramatic increase in the percentage of Sa β -Gal-positive cells at their respective CCPs and maintained the presence of Sa β -Gal-positive

cell under 10% until passage 11 when all lines except Tg#3 start to show a sudden increase in percentage (Figure 9A, B).

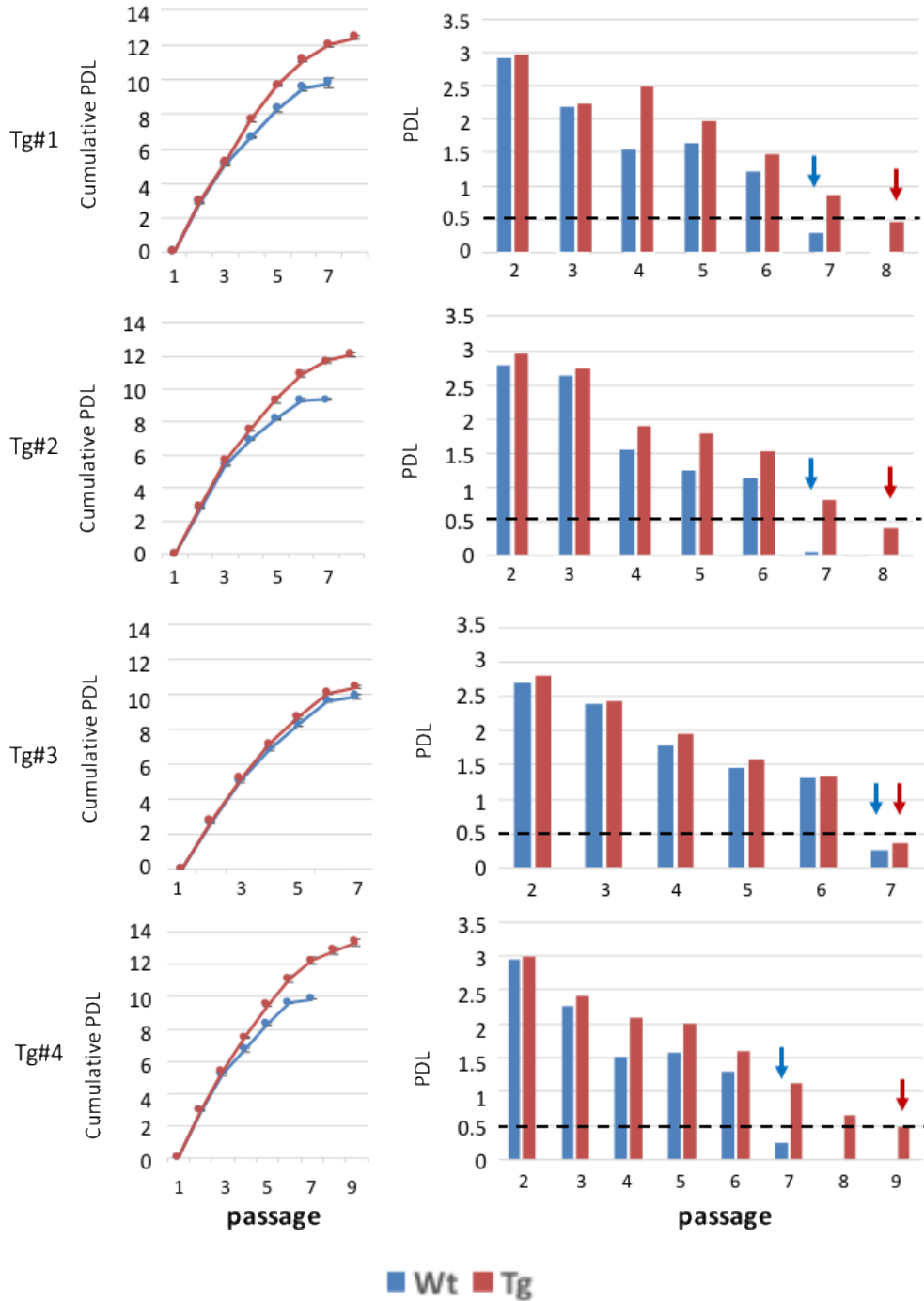


Figure 8: Changes in cell proliferation pattern in MEF cells isolated from *Nampt*-OE transgenic mice. Left panels: growth curves based on cumulative PDLs of each transgenic cell line; right panels: PDL value for each passage from growth curve analysis. Passage with PDL value less than 0.5 threshold (dotted line) is considered to have entered senescence (arrows).

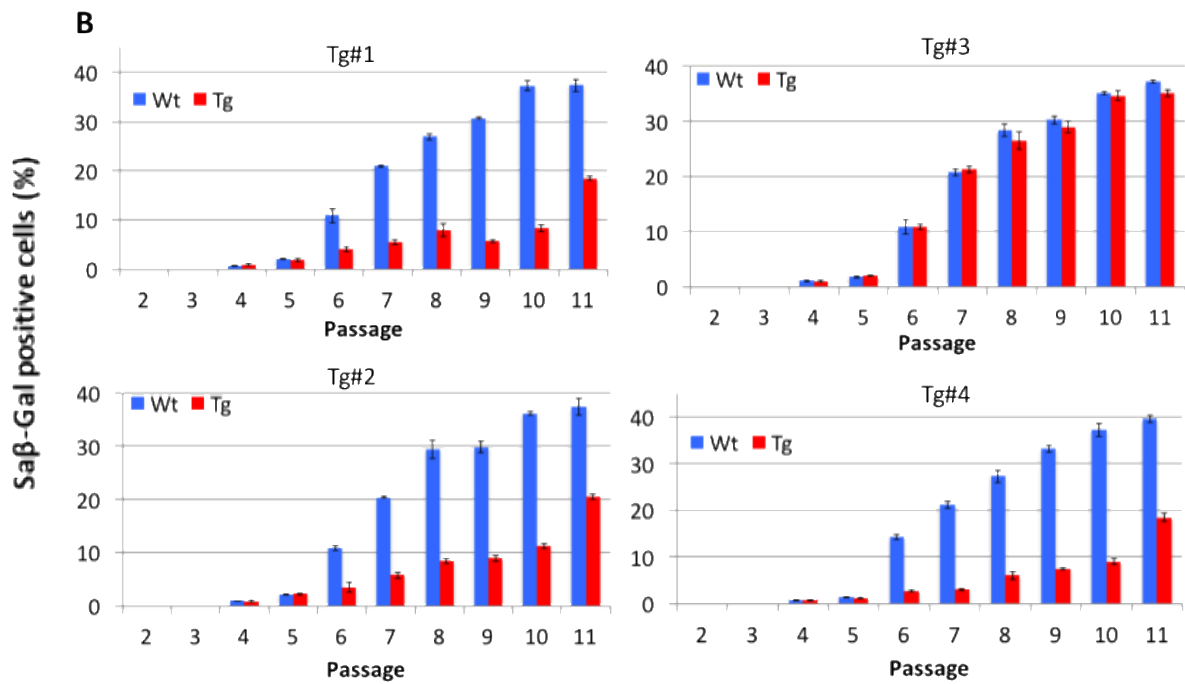
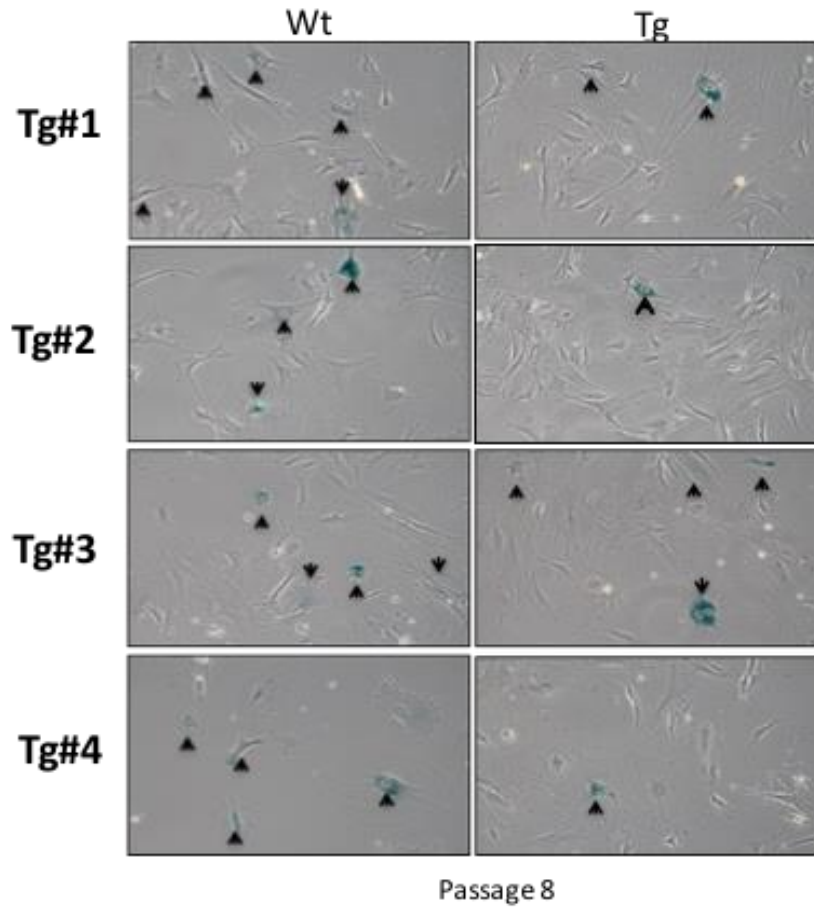


Figure 9: *Nampt*-OE MEF cells have lower presence of senescence cells. (A) Bright field image of senescence-associated β -galactosidase (sa β -Gal) positive cells (arrowhead). (B) Quantitation of Sa β -Gal positive cells in presented in percentage over total cell counted. **: $p < 0.01$.

$p16^{INK4a}$, $p19^{ARF}$ and $p21^{CIP1}$ are well known cell cycle regulators and the expression level of these genes have been known to increase during cellular senescence. To corroborate the Sa β -Gal staining results, we compared the expression level of these markers in cells at passage 4 and 8 as representative of cells at exponential growth and plateaued growth phases, respectively. For these assays, we utilized the Tg#1 and Tg#4 since these two lines have the highest fold in increase in *Nampt* overexpression and elevated NAD⁺ level.

As shown in Figure 10, $p16^{INK4a}$, $p19^{ARF}$ and $p21^{CIP1}$ gene expression levels in *Nampt*-OE cells were observed to be similar to that of wild type cells at passage 4 in Tg#1. However, at passage 8, the expression of these genes in *Nampt*-OE cells was found to be lower than their wild type cells. It is worthy to note that the expression of $p16^{INK4a}$ and $p19^{ARF}$ was upregulated in both wild type and *Nampt*-OE cells at passage 8 when compared to passage 4 while $p21^{CIP1}$ was upregulated at passage 8 only in wild type cells. In Tg#4, $p16^{INK4a}$, $p19^{ARF}$ and $p21^{CIP1}$ gene expression levels in passage 4 were already lower than those in wild type cells and these gene expressions were almost similar between passage 4 and 8. Taken together, these results suggest that *Nampt*-OE cells exhibit a delayed onset of cellular senescence as opposed to wild type MEF cells. This delay could be a contributing factor to the extended cell proliferation phase noted earlier.

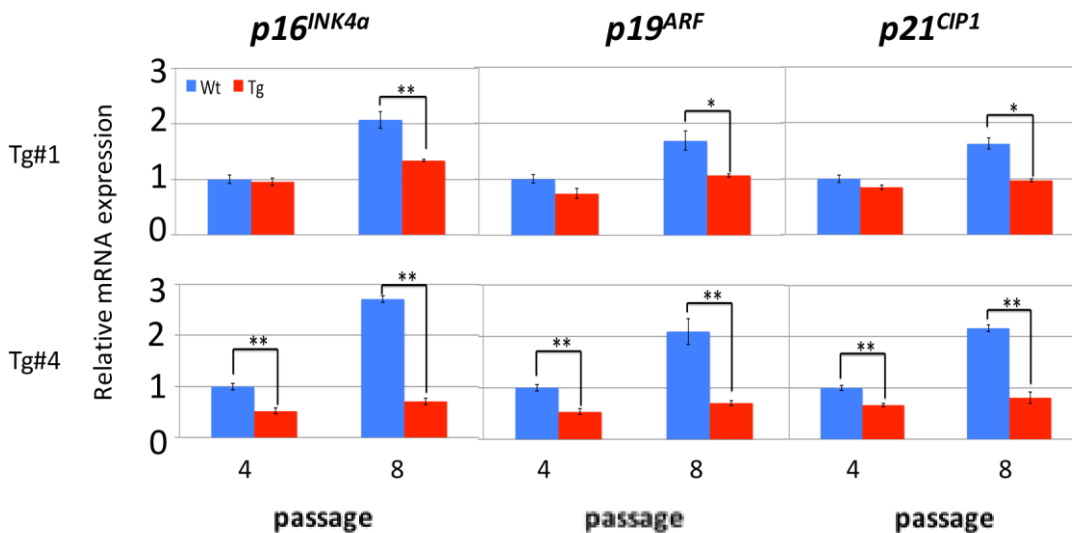


Figure 10: *Nampt*-OE MEF cells have low $p16^{INK4a}$, $p19^{ARF}$ and $p21^{CIP1}$ expression. mRNA level of target genes were normalized to *18s rRNA* gene expression and fold increase calculated were based on the level of wild type (Wt) passage 4 samples. Top panels: Tg#1; bottom panels; Tg#4. *: $p < 0.05$; **: $p < 0.01$.

3.5 *Nampt*-OE cells exhibit higher resistance against oxidative stress and better preservation of cell proliferation potential.

Oxidative stress is one of the more prominent trigger for cellular senescence. It has been found to underlie the premature onset of replicative senescence in cells cultured under hyperoxic (O₂ concentration of ~20%) condition. Therefore, improving resistance towards oxidative stress is likely to be beneficial to stave off senescence onset and preserve cellular proliferation potential. Since our initial results demonstrated that *Nampt*-OE cells have delayed senescence onset compared to wild type MEF cells, we wondered if *Nampt*-OE cells mount a better resistance towards oxidative stress compared to wild type cells.

In order to clarify this, we first measured and compared viability of *Nampt*-OE cells under acute sublethal hydrogen peroxide (H₂O₂) treatment. Cells were treated with an increasing dose of H₂O₂ and these treatments reduced the overall viability of the cells in a dose-dependent manner. However, only Tg#4 with the highest NAMPT overexpression showed a consistent high in viability across the tested H₂O₂ concentrations when compared to wild type MEF cells, while moderate NAMPT overexpression in Tg#1 and #2 only showed significant improvement in viability under the highest H₂O₂ dose. These results suggest that *Nampt*-OE MEF cells have better resistance against oxidative stress (Figure 11).

On top of that, we carried out a cell proliferation assay under chronic low oxidative stress condition. Cells were cultured in the presence of 50μM H₂O₂, and was subcultured every 3 days. From this assay, we observed that *Nampt*-OE cells from all lines have higher cell count as compared to wild type cells. This indicated that under oxidative condition, *Nampt*-OE cells maintain higher proliferation capacity than wild type (Figure 12). Consistent with their levels of the *Nampt* overexpression and NAD⁺ upregulation, *Nampt*-OE MEF cells from Tg#4 showed the highest proliferation potential compared to the rest of the lines based on the cell number recorded at passage 5.

It is interesting to point out that in Tg#3, under oxidative stress condition induced by 50μM H₂O₂ treatment, *Nampt*-OE MEF cells showed a better proliferation potential compared to wild type MEF cells even though cell proliferation was not found to be different under non-stress condition. This indicates that the degree of change in terms of *Nampt* overexpression and NAD⁺ upregulation in Tg#3 MEF cells was not sufficient to

enhance cell proliferation under normal culture condition but can preserve the proliferation potential of wildtype cells under a more intense oxidative stress condition.

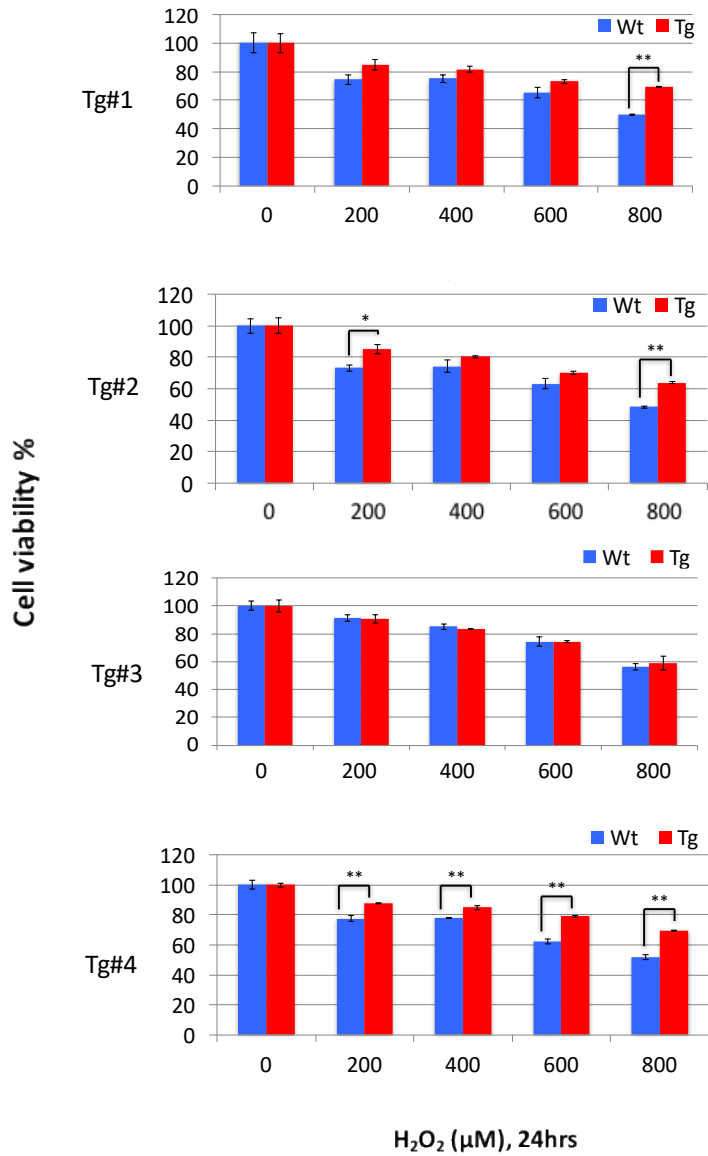


Figure 11: *Nampt*-OE MEF cells have higher viability under acute H₂O₂-induced oxidative stress condition. Cells were treated with H₂O₂ at concentration as described for 24 hours. Cell viability was assessed by counting cells unstained by trypan blue. *: $p < 0.05$; **: $p < 0.01$.

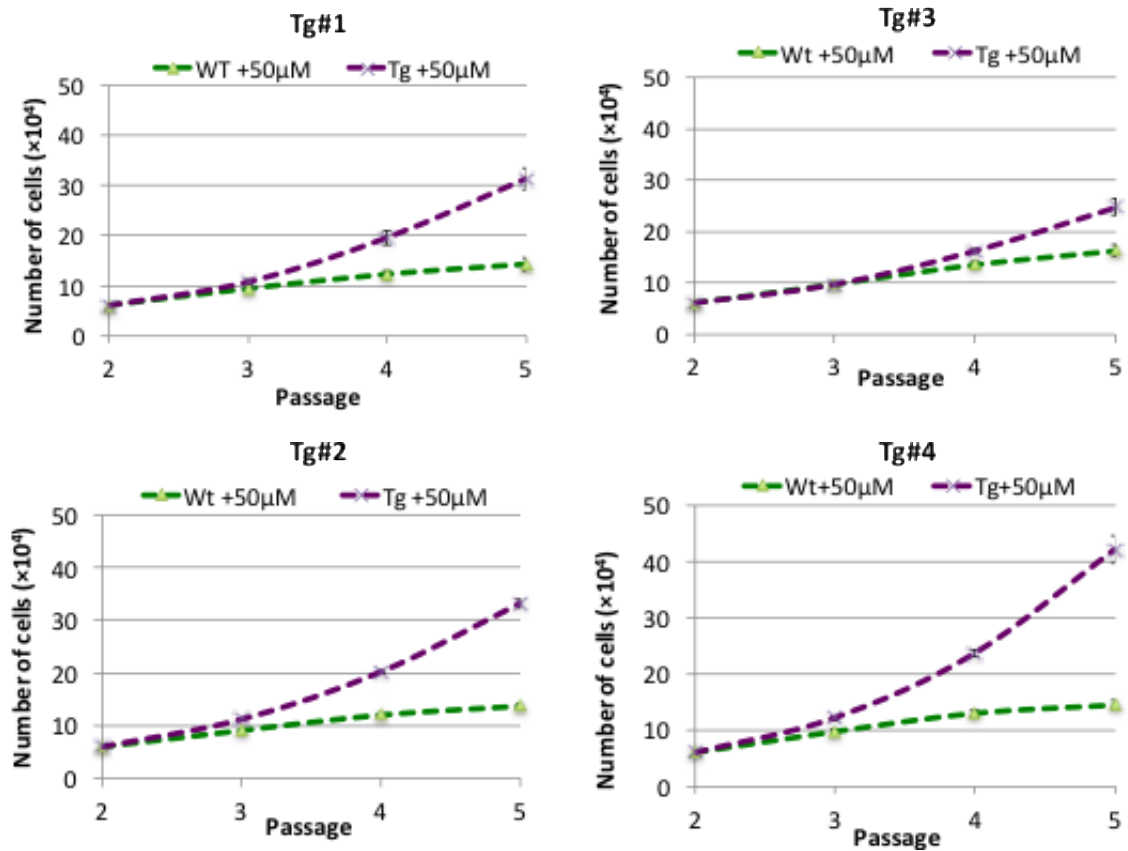


Figure 12: *Nampt*-OE MEF cells have higher proliferative potential under chronic H₂O₂-induced oxidative stress condition. Cells were treated with 50µM H₂O₂. Cell viability was assessed by counting cells unstained by trypan blue. *: $p < 0.05$; **: $p < 0.01$.

3.6 *Nampt*-OE cells exhibit increased ROS scavenging activity

Since *Nampt*-OE cells exhibited enhanced resistance against oxidative stress and higher cell proliferation potential, we wondered if these changes are attributed to an improvement in ROS mitigation. ROS measurement revealed that cellular ROS in *Nampt*-OE cells is 70% lower than the wildtype cells at basal level. And when treated with 100µM H₂O₂, ROS level in both cells showed an increase but ROS level in *Nampt*-OE cells still measured below 50% of that in the wild type MEFs (Figure 13). The low ROS level in *Nampt*-OE cells even under H₂O₂-treated condition suggests that *Nampt*-OE cells has a more active ROS scavenging activity. We wondered if anti-oxidant gene expressions were upregulated in *Nampt*-OE MEF cells. Using qRT-PCR analysis, the results revealed that *Nampt*-OE cells have notable upregulation of *Sod2* and *Catalase* gene expressions, but not *Sod1* and *Gpx1*, when compared to wildtype cells at both

passage 4 and 8, although overall expression level showed a decrease at the later passage (Figure 14). Overall, our results demonstrated that *Nampt*-OE cells have better resistance

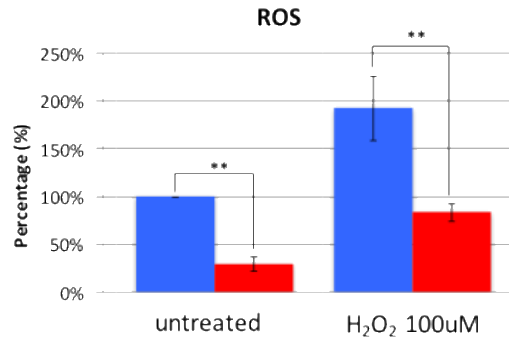


Figure 13: *Nampt*-OE MEF cells have lower ROS levels than wild type MEF cells both under basal and oxidative stress induced by 100 μ M H₂O₂. **:p<0.01.

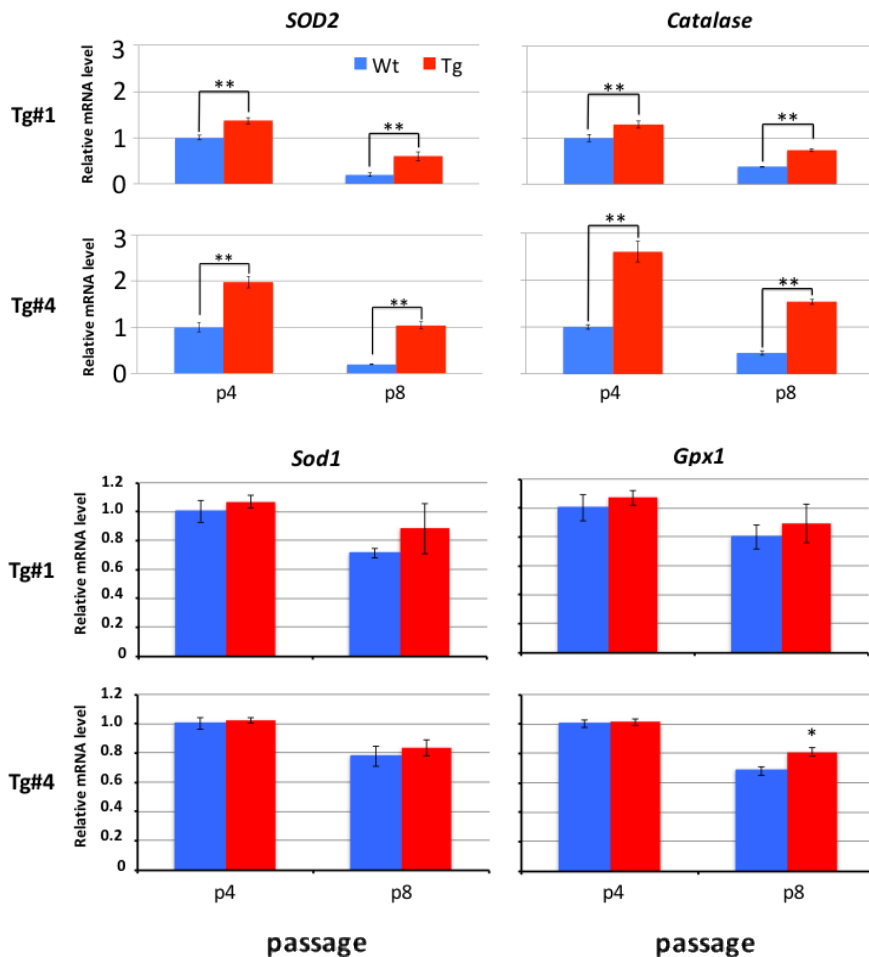


Figure 14: *Nampt*-OE MEF cells have upregulated *SOD2* and *Catalase* gene expression. Total RNA was extracted from primary MEFs at passage 4 and 8 before being subjected to quantitative PCR analysis. Expression level of (A) *Sod2* and *Catalase* and (B) *Sod1* and *Gpx1* were normalized to *18s rRNA* gene expression and the fold increase calculated were based on the level of wild type (Wt) passage 4 samples. *:p<0.05; **:p<0.01

to oxidative stress partly due to enhanced mitigation of ROS and in return show improved proliferative potential than wild type cells.

3.7 *Nampt*-OE cells show increased SIRT1 deacetylase activity

SIRT1 has been shown to regulate cellular proliferation and senescence but this function is dependent on the robustness of the intrinsic NAMPT activity and NAD⁺ level (Ho *et al.*, 2009). SIRT1 is also vital in regulating FOXO-mediated activation of antioxidant enzymes including SOD2 and Catalase (Klotz *et al.*, 2015). Therefore, we tried to find out if the SIRT1 activity is enhanced in response to *Nampt* overexpression.

To that end, SIRT1 activity was measured using the Fluor-de-Lys SIRT1 Fluorometric Kit (Enzo), which is based on the ability of SIRT1 to deacetylate and hence activate a partial p53 protein fused with a fluorescent compound. When fluorescent signals were measured and compared, signal intensity from *Nampt*-OE cells (Tg#4) was found to be 2.5-fold higher than that of the wild type, indicating that *Nampt*-OE cells produced more deacetylated products from the reactions thus suggesting that *Nampt*-OE cells have higher SIRT1 activity than wild type MEF cells (Figure 15). In addition, 1mM NMN treatment did not increase SIRT1 activity. This observation perhaps offers an explanation as to why 1mM NMN treatment was unable to improve cellular proliferation and senescence in wild type MEF cells.

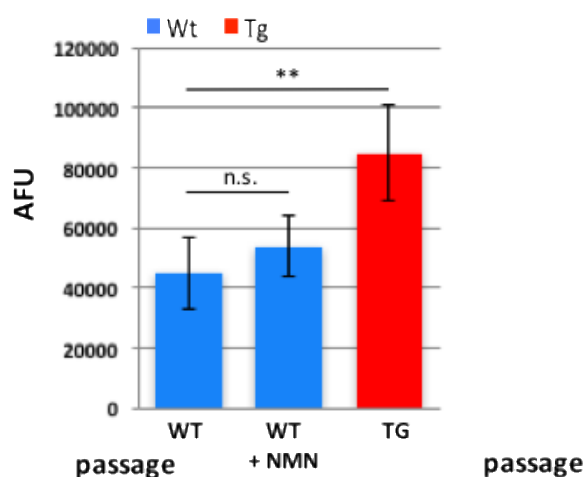


Figure 15: SIRT1 activity is increased in *Nampt*-OE MEF cells. Wild type (WT) cells were cultured with or without 1mM NMN (NAD⁺ precursor) for 24 hours. ** $p < 0.01$; n.s.: not significant when compared to WT.

4.0 Discussions

4.1 NAD⁺ level decreases in passaged MEF cells

Cellular senescence is slowly gaining attention as a key aspect behind the mystery of organismal aging. Growing evidences have implicated cellular senescence process in the early step of tissue degeneration and dysfunction related to aging. The recent findings that identified NAD⁺ as one of the potential determinant for cell longevity have since added another layer of complexity to this conundrum (Gomes *et al.*, 2013). In many examples involving human cells, NAD⁺ and NAMPT levels have been shown to decline both *in vivo* in relation with age and in primary cells that have been extensively passaged during cell culture. In this study, we also observed that NAD⁺ was depleted and NAMPT expression was downregulated in primary MEF cells that have been successively passaged. The consistency of NAMPT-NAD⁺ depletion between human and mouse cell supports the universal role of NAMPT-NAD⁺ in regulating cellular senescence.

The NAD⁺ depletion seen in MEF cells is speculated to be due to several factors. One possible factor is a change in activity of the transcription factors for NAMPT, such as Bmal1-Clock dimer. Bmal1 activity might have declined with age which, in turn, would have caused NAMPT gene downregulation. Another possibility is due to a chronic activation of PARP1 activity that might have exhausted the cellular NAD⁺ reserve. This is because MEF cells were cultured at atmospheric oxygen condition that have been shown to increase oxidative stress and DNA damage accumulation. In addition, depletion of cellular NAD⁺ might also be due to an overactivation of CD38 in senescing MEF cells that consumes NAD⁺ to generate cADPR. This is based on the latest report by Camacho-Pereira (2016) that found CD38 activity was increased and is responsible in age-related decline of NAD⁺.

Furthermore, the NAD⁺-consuming SIRT1 is also found to regulate NAMPT expression to form a positive feedback loop as shown in mouse hepatocytes (Choi *et al.*, 2013). Therefore, the lack of NAD⁺ is also likely to hinder SIRT1 function and disrupt SIRT1-mediated upregulation of NAMPT. This NAMPT/NAD⁺ and SIRT1 interdependency and its conserved effect on cellular senescence between species is consistent with the “NAD world” theory put forth by Imai (2009).

4.2 Supplementation of NMN did not improve cellular proliferation and cellular senescence

We tried to investigate whether any approach to elevate intracellular NAD⁺ level would have an impact on MEF cell proliferation and senescence. First we tried a pharmacological approach to increase NAD⁺ level in MEF cells by supplementing with NMN. However, our results showed that 1mM NMN supplementation did not improve population doubling level despite displaying an increase in the intracellular NAD⁺ level (Figure 2A). Subsequently, we found that SIRT1 activity in NMN-treated MEF cells was not significantly increased (Figure 13). This probably explains why NMN treatment did not impact proliferation and senescence of MEF cells in culture since SIRT1 activity is vital in controlling cellular proliferation and senescence in response to oxidative stress (Furukawa *et al.*, 2007). We speculate that although NMN treatment could increase cellular NAD⁺ level in wild type MEF, it could also result in the accumulation of NAM, the byproduct of NAD⁺ breakdown by SIRT1. NAM is an endogenous inhibitor for SIRT1 and its accumulation would upset the NAD⁺/NAM ratio and favors the inhibition of SIRT1 activity. Of note, it has also been shown that NMN treatment was not able to increase SIRT1 deacetylase activity in myocytes (Hsu *et al.*, 2016) and that SIRT1 gene expression can be downregulated by NMN treatment in primary mouse hepatocytes (Yu *et al.*, 2013). Such accumulation of NAM however might not be present in *Nampt* OE cells. This is because even though *Nampt* overexpression increases NAD⁺ and hence SIRT1 activity, the level of NAM as the byproduct would still be inherently low due to the high *Nampt* activity. In other words, NAMPT OE cells would consistently maintain high NAD⁺ and low NAM state, a condition that would support high SIRT1 activity.

However, previous reports have shown that elevation of NAD⁺ level through exogenous supplementation of NAD⁺ and its intermediates such as NMN and NAM can have positive effects on cell proliferation in human cells. For example, supplementation of NMN to human endothelial cells have been observed to increase NAD⁺ level and preserve proliferation potential from growth inhibition induced by glucose overload (Borradaile *et al.*, 2009). 5mM NAM treatment in normal human fibroblasts, normal keratinocytes and human dermal fibroblasts also have been shown to increase replicative lifespan by at least 1.3-fold (Kang *et al.* 2006), while administration of 0.2mM NAD⁺ to

Hs68 human foreskin fibroblasts can extend cumulative population doubling by two additional passages (Song *et al.*, 2015). Therefore, the inability for NMN to increase MEF cell proliferation suggests that murine cells probably have a different mechanism/preference that mediates the response to exogenous NAD⁺ intermediates. Besides that, this also shows that using *Nampt* overexpression as a means to increase NAD⁺ might be advantageous in circumventing the potential inhibitory effect of NAM accumulation on SIRT1 activity, as opposed to supplementation of NAD⁺ intermediate. Therefore, a more extensive study is much needed to elucidate and confirm why SIRT1 activity is not increased under NMN-induced high NAD⁺ condition.

4.3 *Nampt* overexpression boosts mitochondrial function

Second, we tried to use a genetic approach to increase NAD⁺ level in MEF cells. In particular, we generated transgenic mice that systemically overexpress NAMPT, the rate-limiting enzyme in the NAD⁺ biosynthesis pathway. This transgenic approach potentially allows for the examination of the effect of *Nampt*-OE at the molecular and cellular level, across different developmental stages, across multiple organ and tissue types as well as observation of phenotypic and behavioral changes during natural course of aging. However, this study only focuses on the changes that occurred at the molecular and cellular level.

MEF cells overexpressing *Nampt* have higher NAD⁺ level compared to wild type MEF cells and are able to sustain the increase considerably in later passages. Due to the interdependence of redox reactions and intracellular NAD⁺ concentration and/or a possible autoregulation mechanism since NAMPT activity requires ATP, increased NAD⁺ level in *Nampt*-OE MEF cells showed a concomitant increase in ATP synthesis (Figure 5A). For example, we observed a 1.3-fold increase in ATP when NAD⁺ is increased 1.3-fold in Tg#3. Similarly, it has been shown that a 1.19-fold increase in ATP when NAD⁺ is increased 1.3-fold by a localized *Nampt* overexpression in cardiac muscles (Hsu *et al.* 2009). This increase in activity however was not accompanied by any change in mitochondrial mass based on the unchanged level of mitochondrial membrane protein VDAC (Figure 5C).

4.4 NAMPT overexpressing cells show higher proliferation doubling capability due to improved oxidative stress mitigation

Here, we provide evidences that *Nampt* overexpression have a positive impact on cellular oxidative stress mitigation, proliferation and senescence onset of MEF cells maintained under cell culture condition. MEF cells overexpressing *Nampt* was found to have enhanced antioxidant activity that lowered ROS level and conferred better resistance towards acute and chronic oxidative assaults as well as preserving the cellular proliferation potential (Figure 9, 10).

We postulate that the activation of SIRT1 function is central in modulating these effects. SIRT1 activity is highly dependent on NAD⁺ level and *Nampt* overexpression in human smooth muscle cells have been demonstrated to boost SIRT1 activity in promoting resistance to senescence and extension of replicative lifespan (Ho *et al.*, 2009). Consistent with this, SIRT1 activation was also observed in *Nampt*-OE MEF cells, presumably as a result of increased intracellular NAD⁺ level (Figure 13). SIRT1 regulates the activity and function of many proteins essential for metabolic homeostasis and cell survival. Among the enzymes that fall under SIRT1 regulation are the primary antioxidant enzymes SOD2 and Catalase through the function of FOXO family transcription factors (Kops *et al.*, 2002). Gene expressions of *Sod2* and *Catalase* have been shown to be activated in astrocyte after SIRT1 upregulation (Cheng *et al.*, 2014). Mice with specific loss of SOD2 function in the connective tissues suffered premature onset of age-related phenotypes such as kyphosis and skin atrophy along with reduced overall lifespan (Treiber *et al.*, 2011). Meanwhile, specific Catalase overexpression in the mitochondria have been shown to extend mouse lifespan (Schriner *et al.*, 2006). *Sod2* and *Catalase* upregulation in *Nampt*-OE MEF cells therefore provides a cohesive proof that supports the impact *Nampt* overexpression had on oxidative stress mitigation (Figure 12). Not only *Sod2* gene expression, but also SOD2 scavenge activity might be increased in *Nampt*-OE MEF cells, since SIRT3, another Sirtuin family deacetylase located in mitochondria, has been demonstrated to deacetylate SOD2 and enhance its activity, thereby reducing oxidative stress (Qiu *et al.*, 2010; Chen, *et al.*, 2011).

Accordingly, expression of *p16^{INK4a}*, *p19^{ARF}* and *p21^{CIP1}* genes, that would be upregulated upon activation of DNA damage signals by oxidative stress, were found to be more subdued in *Nampt*-OE MEF cells when compared to wild type MEF cells,

indicating that the level of DNA damage stress is not at a critical level (Figure 8). The level of repression of these genes were dependent on the *Nampt* overexpression level since significant downregulation was observed in both passage 4 and 8 only in Tg#4 which has the highest *Nampt* overexpression. Our results also show the upregulation of all three markers at passage 8, suggesting that MEF cells engage both p19^{ARF}-p53-p21^{CIP1} arm and p16^{INK4a}-pRb arm of the senescence activation pathway. This indicated that senescence activation in MEF cells is a tightly regulated process. Furthermore, activation of both arms of senescence activation pathway in this case is potentially vital in demonstrating the increased resistance of *Nampt*-OE MEF cells towards both acute and chronic oxidative stress. This is because MEF have shown to be dependent on p19^{ARF} to initiate senescence under chronic DNA damage while p53 response towards acute DNA damage is found to be p19^{ARF} independent (Biegging-Rolett *et al.*, 2016). It is interesting to note that in MEF cell undergoing senescence, p53 level was previously reported to remain unchanged (Kim *et al.*, 2002). Attempts have been made to compare the level of p53 in wild type and *Nampt*-OE MEF cells but to no avail. It is noted that information comparing p53 levels in these cells would further substantiate the effect *Nampt*-OE has on delaying the onset of cellular senescence.

Nampt-OE MEF cells were observed to have a higher population doubling capacity and a delayed cell cycle arrest of 1-2 passages later than wild type MEF cells. Interestingly, this arrest is not completely consistent with Sa β -Gal staining results because Tg#4 MEF cells showed low accumulation of Sa β -Gal positive cells at the point of proliferation arrest (passage 8) as compared to wild type MEF cells that had dramatic increase of Sa β -Gal positive cells at the point of proliferation arrest (passage 6). In fact, Tg#4 MEF cells showed a dramatic increase in Sa β -Gal positive cells percentage at passage 11 (Figure 7). This suggests that Tg#4 MEF cells were arrested by p16^{INK4a}, p19^{ARF} and p21^{CIP1} activation of cell cycle checkpoints and probably kept under quiescent state rather than becoming senescent at passage 8. Quiescent state is known to precede senescence event (Blagosklonny, 2011). And based on the Sa β -Gal staining, Tg#4 MEF cells were maintained in arrested state longer than wild type cells before eventually becoming senescent. These events are similar with arrested retinal pigmental epithelium (ARPE-19) cells that were treated with rapamycin, an mTOR pathway inhibitor (Demidenko *et al.*, 2009). Arrested ARPE-19 cells that have suppressed mTOR activity

showed extended quiescent state that precedes senescence. Therefore, it is likely that *Nampt* overexpression prolonged the duration of this quiescent state in MEF cells, effectively protecting them from becoming irreversibly arrested or senescent.

This protective effect of *Nampt* overexpression might be achieved through SIRT1-mediated increase in mTOR inhibitor complex TSC2 activity (Ghosh *et al.*, 2010), as our data showed that SIRT1 activity was increased in *Nampt*-OE MEF cells. Similar protective effect of *Nampt* overexpression was reported in neuronal cells during cerebral ischemia (Wang *et al.*, 2012). Further examination into the activity of mTOR in both wild type and *Nampt*-OE MEF cells is required to elucidate potential relationship between *Nampt* overexpression and the regulation of mTOR pathway.

5.0 Concluding remarks

In this study, we attempted to shed some light onto the mechanism of cellular senescence in MEF cells in association with NAMPT and NAD⁺-dependent functions. *Nampt* overexpression in MEF cells resulted in the increase in NAD⁺ level which in turn increased SIRT1 activity. Higher SIRT1 activity promotes delay onset of senescence during culture through enhancing resistance to oxidative stress. Supplementation of NAMPT enzymatic product NMN to wild type MEF cells however have no effect on the onset of senescence despite increasing NAD⁺ level. This supports the growing notion that NAMPT and NAD⁺ levels play a role in determining the decision-making for cellular proliferation vs. senescence both in human and mouse cells.

Moving forward, more aspects of NAMPT regulation on MEF cell proliferation and senescence should be addressed and elucidated. NAMPT and SIRT1 form an auto feedback loop with *Bmal1*, connecting cellular metabolism and the circadian mechanism. And interestingly, cellular senescence has been implicated with altering circadian clock gene expression (Kunieda *et al.* 2006). Therefore, *Nampt* overexpression could have an impact on the modulation of the cellular circadian oscillation mechanism. It is thus possible that the circadian oscillation mechanism partly contributes to the delayed senescence observed in *Nampt*-OE MEF cells.

Aside from that, the open question regarding the NAM/NAD⁺ ratio in *Nampt*-OE MEF cells needs further clarification. NAMPT produce NMN (and later generate NAD⁺) by consuming NAM. Therefore, constitutive *Nampt*-OE would likely depletes NAM pool. Low NAM level might be advantageous since NAM is an endogenous SIRT1 inhibitor. However, NAM can also be methylated by NNMT to form N-methylnicotinamide (MNAM). MNAM has been demonstrated to stabilize SIRT1 by regulating its ubiquitin-proteasome degradation (Hong *et al.*, 2015). It is therefore intriguing to see how *Nampt*-OE augment the interplay between NAD⁺/NAM/MNAM in MEF cells.

Finally, it would be of utmost interest to see how the systemic NAMPT overexpression would impact the healthy lifespan or 'healthspan' and median lifespan of the transgenic mice. Baker and colleagues have demonstrated earlier the advantage of removing p16^{INK4a}-positive senescent cell on the onset of age-related diseases as well as on median lifespan in mice (Baker *et al.*, 2011; 2016). So far, no morphological difference

was observed when NAMPT is overexpressed in the murine heart when compared to wild type mice (Hsu *et al.*, 2009; Frederick *et al.*, 2015). However, given that *p16^{INK4a}* expression in MEF cells was downregulated and senescent cell occurrence was delayed when NAMPT is overexpressed, we are positive that NAMPT overexpression would also have similar positive effect on organismal healthspan and lifespan extension.

6.0 Acknowledgement

I wish to express my utmost gratitude to Prof. Yasumasa Bessho, for his kind guidance, support, and patience throughout this study and my stay in the lab. My sincere gratitude to Prof. Jun-ya Kato and Prof. Kenji Kohno for their invaluable comments and advices as Doctoral supervising committee members throughout this study as well as Assoc. Prof. Dr. Yasumasa Ishida for reviewing this thesis. I am very grateful to Dr. Yasukazu Nakahata, Dr. Takaaki Matsui, Dr. Norihiro Ishida-Kitagawa and all members of Laboratory of Gene Regulation Research – NAIST for their continuous supports, technical assistance, fruitful discussions and for the friendship and enjoyable company. I would like to thank the Ministry of Education, Culture, Sports, Science and Technology of Japan for providing me with the education opportunity and financial support through the NAIST Global COE Program. And lastly to my family and friends for their love, support, and encouragement throughout this journey.

7.0 References

- Bai, P., Cantó, C., Oudart, H., Brunyánszki, A., Cen, Y., Thomas, C., ... & Schoonjans, K. (2011). PARP-1 inhibition increases mitochondrial metabolism through SIRT1 activation. *Cell metabolism*, 13(4), 461-468.
- Baker, D. J., Wijshake, T., Tchkonina, T., LeBrasseur, N. K., Childs, B. G., Van De Sluis, B., ... & van Deursen, J. M. (2011). Clearance of p16Ink4a-positive senescent cells delays ageing-associated disorders. *Nature*, 479(7372), 232-236.
- Baker, D. J., Childs, B. G., Durik, M., Wijers, M. E., Sieben, C. J., Zhong, J., ... & Khazaie, K. (2016). Naturally occurring p16Ink4a-positive cells shorten healthy lifespan. *Nature*, 530(7589), 184-189.
- Barbosa, M. T. P., Soares, S. M., Novak, C. M., Sinclair, D., Levine, J. A., Aksoy, P., & Chini, E. N. (2007). The enzyme CD38 (a NAD glycohydrolase, EC 3.2. 2.5) is necessary for the development of diet-induced obesity. *The FASEB Journal*, 21(13), 3629-3639.
- Bekaert, S., Derradji, H., & Baatout, S. (2004). Telomere biology in mammalian germ cells and during development. *Developmental biology*, 274(1), 15-30.
- Ben-Porath, I., & Weinberg, R. A. (2005). The signals and pathways activating cellular senescence. *The international journal of biochemistry & cell biology*, 37(5), 961-976.
- Biegging-Rolett, K. T., Johnson, T. M., Brady, C. A., Beaudry, V. G., Pathak, N., Han, S., & Attardi, L. D. (2016). p19Arf is required for the cellular response to chronic DNA damage. *Oncogene*.
- Blagosklonny, M. V. (2012). Cell cycle arrest is not yet senescence, which is not just cell cycle arrest: terminology for TOR-driven aging. *Aging (Albany NY)*, 4(3), 159-165.
- Borradaile, N. M., & Pickering, J. G. (2009). Nicotinamide phosphoribosyltransferase imparts human endothelial cells with extended replicative lifespan and enhanced angiogenic capacity in a high glucose environment. *Aging cell*, 8(2), 100-112.
- Braidy, N., Guillemin, G. J., Mansour, H., Chan-Ling, T., Poljak, A., & Grant, R. (2011). Age related changes in NAD⁺ metabolism oxidative stress and Sirt1 activity in wistar rats. *PloS one*, 6(4), e19194.
- Busuttill, R. A., Rubio, M., Dollé, M. E., Campisi, J., & Vijg, J. (2003). Oxygen accelerates the accumulation of mutations during the senescence and immortalization of murine cells in culture. *Aging cell*, 2(6), 287-294.

- Camacho-Pereira, J., Tarrago, M. G., Chini, C. C., Nin, V., Escande, C., Warner, G. M., ... & Chini, E. N. (2016). CD38 Dictates Age-Related NAD Decline and Mitochondrial Dysfunction through an SIRT3-Dependent Mechanism. *Cell Metabolism*, 23(6), 1127-1139.
- Cantó, C., Houtkooper, R. H., Pirinen, E., Youn, D. Y., Oosterveer, M. H., Cen, Y., Fernandez-Marcos, P., J., Yamamoto, H., Andreux, P., A., Cettour-Rose, P., Gademann, K., Rinsch, C., Schoonjans, K., Sauve, A. A., & Auwerx, J. (2012). The NAD⁺ precursor nicotinamide riboside enhances oxidative metabolism and protects against high-fat diet-induced obesity. *Cell metabolism*, 15(6), 838-847.
- Chang, J., Wang, Y., Shao, L., Laberge, R. M., Demaria, M., Campisi, J., ... & Luo, Y. (2016). Clearance of senescent cells by ABT263 rejuvenates aged hematopoietic stem cells in mice. *Nature medicine*, 22(1), 78-83.
- Chen, Y., Zhang, J., Lin, Y., Lei, Q., Guan, K. L., Zhao, S., & Xiong, Y. (2011). Tumour suppressor SIRT3 deacetylates and activates manganese superoxide dismutase to scavenge ROS. *EMBO reports*, 12(6), 534-541.
- Cheng, Y., Takeuchi, H., Sonobe, Y., Jin, S., Wang, Y., Horiuchi, H., ... & Suzumura, A. (2014). Sirtuin 1 attenuates oxidative stress via upregulation of superoxide dismutase 2 and catalase in astrocytes. *Journal of neuroimmunology*, 269(1), 38-43.
- Choi, S. E., Fu, T., Seok, S., Kim, D. H., Yu, E., Lee, K. W., ... & Kemper, J. K. (2013). Elevated microRNA - 34a in obesity reduces NAD⁺ levels and SIRT1 activity by directly targeting NAMPT. *Aging cell*, 12(6), 1062-1072.
- Coppe, J., Patil, C. K., Rodier, F., Sun, Y., Munoz, D. P., Goldstein, J., Nelson, P. S., Desprez, P., & Campisi, J. (2008). Senescence-associated secretory phenotypes reveal cell-nonautonomous functions of oncogenic RAS and the p53 tumor suppressor. *PLoS Biol* 6(12), 2853-2868.
- De Figueiredo, L. F., Gossmann, T. I., Ziegler, M., & Schuster, S. (2011). Pathway analysis of NAD⁺ metabolism. *Biochemical Journal*, 439(2), 341-348.
- Debacq-Chainiaux, F., Erusalimsky, J. D., Campisi, J., & Toussaint, O. (2009). Protocols to detect senescence-associated beta-galactosidase (SA- β gal) activity, a biomarker of senescent cells in culture and in vivo. *Nature protocols*, 4(12), 1798-1806.
- Demidenko, Z. N., Zubova, S. G., Bukreeva, E. I., Pospelov, V. A., Pospelova, T. V., & Blagosklonny, M. V. (2009). Rapamycin decelerates cellular senescence. *Cell cycle*, 8(12), 1888-1895.
- Fischer, B., & Bavister, B. D. (1993). Oxygen tension in the oviduct and uterus of rhesus monkeys, hamsters and rabbits. *Journal of reproduction and fertility*, 99(2), 673-679.

- Frederick, D. W., Davis, J. G., Dávila, A., Agarwal, B., Michan, S., Puchowicz, M. A., ... & Baur, J. A. (2015). Increasing NAD synthesis in muscle via nicotinamide phosphoribosyltransferase is not sufficient to promote oxidative metabolism. *Journal of Biological Chemistry*, 290(3), 1546-1558.
- Furukawa, A., Tada-Oikawa, S., Kawanishi, S., & Oikawa, S. (2007). H₂O₂ accelerates cellular senescence by accumulation of acetylated p53 via decrease in the function of SIRT1 by NAD⁺ depletion. *Cellular Physiology and Biochemistry*, 20(1-4), 045-054.
- Ghosh, H. S., McBurney, M., & Robbins, P. D. (2010). SIRT1 negatively regulates the mammalian target of rapamycin. *PloS one*, 5(2), e9199.
- Gomes, A. P., Price, N. L., Ling, A. J., Moslehi, J. J., Montgomery, M. K., Rajman, L., ... & Mercken, E. M. (2013). Declining NAD⁺ induces a pseudohypoxic state disrupting nuclear-mitochondrial communication during aging. *Cell*, 155(7), 1624-1638.
- Gorbunova, V., & Seluanov, A. (2009). Coevolution of telomerase activity and body mass in mammals: from mice to beavers. *Mechanisms of ageing and development*, 130(1), 3-9.
- Harvey, D. M., & Levine, A. J. (1991). p53 alteration is a common event in the spontaneous immortalization of primary BALB/c murine embryo fibroblasts. *Genes & development*, 5(12b), 2375-2385.
- Hausmann, M. F., Winkler, D. W., Huntington, C. E., Nisbet, I. C., & Vleck, C. M. (2007). Telomerase activity is maintained throughout the lifespan of long-lived birds. *Experimental gerontology*, 42(7), 610-618.
- Ho, C., van der Veer, E., Akawi, O., & Pickering, J. G. (2009). SIRT1 markedly extends replicative lifespan if the NAD⁺ salvage pathway is enhanced. *FEBS letters*, 583(18), 3081-3085.
- Hong, S., Moreno-Navarrete, J. M., Wei, X., Kikukawa, Y., Tzamei, I., Prasad, D., ... & Pissios, P. (2015). Nicotinamide N-methyltransferase regulates hepatic nutrient metabolism through Sirt1 protein stabilization. *Nature medicine*, 21(8), 887-894.
- Hsu, C. P., Oka, S., Shao, D., Hariharan, N., & Sadoshima, J. (2009). Nicotinamide phosphoribosyltransferase regulates cell survival through NAD⁺ synthesis in cardiac myocytes. *Circulation research*, 105(5), 481-491.
- Imai, S. I. (2009). The NAD World: a new systemic regulatory network for metabolism and aging—Sirt1, systemic NAD biosynthesis, and their importance. *Cell biochemistry and biophysics*, 53(2), 65-74.
- Imai, S. I., & Guarente, L. (2014). NAD⁺ and sirtuins in aging and disease. *Trends in cell biology*, 24(8), 464-471.

- Jang, S. Y., Kang, H. T., & Hwang, E. S. (2012). Nicotinamide-induced mitophagy event mediated by high NAD⁺/NADH ratio and SIRT1 protein activation. *Journal of Biological Chemistry*, 287(23), 19304-19314.
- Itahana, K., Campisi, J., & Dimri, G. P. (2004). Mechanisms of cellular senescence in human and mouse cells. *Biogerontology*, 5(1), 1-10.
- Johmura, Y., Shimada, M., Misaki, T., Naiki-Ito, A., Miyoshi, H., Motoyama, N., Ohtani, N., Hara, E., Nakamura, M., Morita, A., Takahashi, S., & Nakanishi M. (2014). Necessary and sufficient role for a mitosis skip in senescence induction. *Molecular cell*, 55(1), 73-84.
- Jozefczuk, J., Drews, K., & Adjaye, J. (2012). Preparation of mouse embryonic fibroblast cells suitable for culturing human embryonic and induced pluripotent stem cells. *JoVE (Journal of Visualized Experiments)*, (64), e3854-e3854.
- Kamijo, T., Zindy, F., Roussel, M. F., Quelle, D. E., Downing, J. R., Ashmun, R. A., ... & Sherr, C. J. (1997). Tumor suppression at the mouse INK4a locus mediated by the alternative reading frame product p19 ARF. *Cell*, 91(5), 649-659.
- Kang, H. T., Lee, H. I., & Hwang, E. S. (2006). Nicotinamide extends replicative lifespan of human cells. *Aging cell*, 5(5), 423-436.
- Kim, H., You, S., Farris, J., Kong, B. W., Christman, S. A., Foster, L. K., & Foster, D. N. (2002). Expression profiles of p53-, p16 INK4a-, and telomere-regulating genes in replicative senescent primary human, mouse, and chicken fibroblast cells. *Experimental cell research*, 272(2), 199-208.
- Klement, K., & Goodarzi, A. A. (2014). DNA double strand break responses and chromatin alterations within the aging cell. *Experimental cell research*, 329(1), 42-52.
- Klotz, L. O., Sánchez-Ramos, C., Prieto-Arroyo, I., Urbánek, P., Steinbrenner, H., & Monsalve, M. (2015). Redox regulation of FoxO transcription factors. *Redox biology*, 6, 51-72.
- Koltai, E., Szabo, Z., Atalay, M., Boldogh, I., Naito, H., Goto, S., ... & Radak, Z. (2010). Exercise alters SIRT1, SIRT6, NAD and NAMPT levels in skeletal muscle of aged rats. *Mechanisms of ageing and development*, 131(1), 21-28.
- Kops, G. J., Dansen, T. B., Polderman, P. E., Saarloos, I., Wirtz, K. W., Coffey, P. J., ... & Burgering, B. M. (2002). Forkhead transcription factor FOXO3a protects quiescent cells from oxidative stress. *Nature*, 419(6904), 316-321.
- Kuilman, T., & Peeper, D. S. (2009). Senescence-messaging secretome: SMS-ing cellular stress. *Nature Reviews Cancer*, 9(2), 81-94.

- Kunieda, T., Minamino, T., Katsuno, T., Tateno, K., Nishi, J. I., Miyauchi, H., ... & Komuro, I. (2006). Cellular senescence impairs circadian expression of clock genes in vitro and in vivo. *Circulation research*, 98(4), 532-539.
- Kurosawa, H., Kimura, M., Noda, T., & Amano, Y. (2006). Effect of oxygen on in vitro differentiation of mouse embryonic stem cells. *Journal of bioscience and bioengineering*, 101(1), 26-30.
- Lee, B. Y., Han, J. A., Im, J. S., Morrone, A., Johung, K., Goodwin, E. C., Kleijer, W. J., DiMaio, D., & Hwang, E. S. (2006). Senescence-associated β -galactosidase is lysosomal β -galactosidase. *Aging cell*, 5(2), 187-195.
- Lim, C., Potts, M., & Helm, R. F. (2006). Nicotinamide extends the replicative life span of primary human cells. *Mechanism of Ageing and Development*, 127(6), 511-514.
- Liu, D., Pitta, M., Jiang, H., Lee, J. H., Zhang, G., Chen, X., Kawamoto, E., M., & Mattson, M. P. (2013). Nicotinamide forestalls pathology and cognitive decline in Alzheimer mice: evidence for improved neuronal bioenergetics and autophagy procession. *Neurobiology of aging*, 34(6), 1564-1580.
- Mao, Z., Ke, Z., Gorbunova, V., & Seluanov, A. (2012). Replicatively senescent cells are arrested in G1 and G2 phases. *Aging*, 4(6), 431-5.
- Massudi, H., Grant, R., Braidy, N., Guest, J., Farnsworth, B., & Guillemin, G. J. (2012). Age-associated changes in oxidative stress and NAD⁺ metabolism in human tissue. *PLoS One*, 7(7), e42357.
- Mouchiroud, L., Houtkooper, R. H., Moullan, N., Katsyuba, E., Ryu, D., Cantó, C., ... & Guarente, L. (2013). The NAD⁺/sirtuin pathway modulates longevity through activation of mitochondrial UPR and FOXO signaling. *Cell*, 154(2), 430-441.
- Nakahata, Y., Sahar, S., Astarita, G., Kaluzova, M., & Sassone-Corsi, P. (2009). Circadian control of the NAD⁺ salvage pathway by CLOCK-SIRT1. *Science*, 324(5927), 654-657.
- Narita, M., Nuñez, S., Heard, E., Narita, M., Lin, A. W., Hearn, S. A., Spector, D. L., Hannon, G. J., & Lowe, S. W. (2003). Rb-mediated heterochromatin formation and silencing of E2F target genes during cellular senescence. *Cell*, 113(6), 703-716.
- Naylor, R. M., Baker, D. J., & Deursen, J. M. (2013). Senescent cells: a novel therapeutic target for aging and age-related diseases. *Clinical Pharmacology & Therapeutics*, 93(1), 105-116.
- Parrinello, S., Samper, E., Krtolica, A., Goldstein, J., Melov, S., & Campisi, J. (2003). Oxygen sensitivity severely limits the replicative lifespan of murine fibroblasts. *Nature cell biology*, 5(8), 741-747.

- Pittelli, M., Formentini, L., Faraco, G., Lapucci, A., Rapizzi, E., Cialdai, F., Romano, G., Moneti, G., Moroni, F., & Chiarugi, A. (2010). Inhibition of Nicotinamide Phosphoribosyltransferase: Cellular Bioenergetics Reveals A Mitochondrial Insensitive Nad Pool. *Journal of Biological Chemistry*, 285(44), 34106-34114.
- Qiu, X., Brown, K., Hirschey, M. D., Verdin, E., & Chen, D. (2010). Calorie restriction reduces oxidative stress by SIRT3-mediated SOD2 activation. *Cell metabolism*, 12(6), 662-667.
- Revollo, J. R., Grimm, A. A., & Imai, S. (2004). The NAD biosynthesis pathway mediated by Nicotinamide Phosphoribosyltransferase regulates Sir2 activity in mammalian cells. *J Biol Chem* 279(49), 50754-50763.
- Ruggieri, S., Orsomando, G., Sorci, L., & Raffaelli, N. (2015). Regulation of NAD biosynthetic enzymes modulates NAD-sensing processes to shape mammalian cell physiology under varying biological cues. *Biochimica et Biophysica Acta (BBA)-Proteins and Proteomics*, 1854(9), 1138-1149.
- Scheibye-Knudsen, M., Mitchell, S. J., Fang, E. F., Iyama, T., Ward, T., Wang, J., Dunn, C. A., Singh, N., Weith, S., Hasan-Olive, M. M., Mangerich, A., Wilson, M. A., Mattson, M. P., Bergersen, L. H., Cogger, V. C., Warren, A., Le Couteur, Moaddel, Wilson, Croteau, D. L., de Cabo, R., & Bohr, V. A. (2014). A high-fat diet and NAD⁺ activate Sirt1 to rescue premature aging in cockayne syndrome. *Cell metabolism*, 20(5), 840-855.
- Schriner, S. E., Linford, N. J., Martin, G. M., Treuting, P., Ogburn, C. E., Emond, M., ... & Wallace, D. C. (2005). Extension of murine life span by overexpression of catalase targeted to mitochondria. *science*, 308(5730), 1909-1911.
- Sedelnikova, O. A., Horikawa, I., Zimonjic, D. B., Popescu, N. C., Bonner, W. M., & Barrett, J. C. (2004). Senescing human cells and ageing mice accumulate DNA lesions with unreparable double-strand breaks. *Nature cell biology*, 6(2), 168-170.
- Shawi, M., & Autexier, C. (2008). Telomerase, senescence and ageing. *Mechanisms of ageing and development*, 129(1), 3-10
- Shay, J. W., & Wright, W. E. (2000). Telomere dynamics in cancer progression and prevention: fundamental differences in human and mouse telomere biology. *Nat Med*, 6, 849-851.
- Smogorzewska, A., & de Lange, T. (2002). Different telomere damage signaling pathways in human and mouse cells. *The EMBO journal*, 21(16), 4338-4348.
- Song, T. Y., Yeh, S. L., Hu, M. L., Chen, M. Y., & Yang, N. C. (2015). A Nampt inhibitor FK866 mimics vitamin B3 deficiency by causing senescence of human fibroblastic Hs68 cells via attenuation of NAD⁺-SIRT1 signaling. *Biogerontology*, 16(6), 789-800.

- Stein, L. R., & Imai, S. I. (2014). Specific ablation of Nampt in adult neural stem cells recapitulates their functional defects during aging. *The EMBO journal*, 33(12), 1321-1340.
- Treiber, N., Maity, P., Singh, K., Kohn, M., Keist, A. F., Ferchiu, F., ... & Kochanek, S. (2011). Accelerated aging phenotype in mice with conditional deficiency for mitochondrial superoxide dismutase in the connective tissue. *Aging cell*, 10(2), 239-254.
- Tsai, S. B., Tucci, V., Uchiyama, J., Fabian, N. J., Lin, M. C., Bayliss, P. E., ... & Kishi, S. (2007). Differential effects of genotoxic stress on both concurrent body growth and gradual senescence in the adult zebrafish. *Aging cell*, 6(2), 209-224.
- van der Veer, E., Ho, C., O'Neil, C., Barbosa, N., Scott, R., Cregan, S. P., & Pickering, J. G. (2007). Extension of human cell lifespan by nicotinamide phosphoribosyltransferase. *Journal of Biological Chemistry*, 282(15), 10841-10845.
- Venkatesan, R. N., & Price, C. (1998). Telomerase expression in chickens: constitutive activity in somatic tissues and down-regulation in culture. *Proceedings of the National Academy of Sciences*, 95(25), 14763-14768.
- Wang, P., Guan, Y. F., Du, H., Zhai, Q. W., Su, D. F., & Miao, C. Y. (2012). Induction of autophagy contributes to the neuroprotection of nicotinamide phosphoribosyltransferase in cerebral ischemia. *Autophagy*, 8(1), 77-87.
- Yang, N. C., Song, T. Y., Chang, Y. Z., Chen, M. Y., & Hu, M. L. (2015). Up-regulation of nicotinamide phosphoribosyltransferase and increase of NAD⁺ levels by glucose restriction extend replicative lifespan of human fibroblast Hs68 cells. *Biogerontology*, 16(1), 31-42.
- Yoshino, J., Mills, K. F., Yoon, M. J., & Imai, S. I. (2011). Nicotinamide mononucleotide, a key NAD⁺ intermediate, treats the pathophysiology of diet-and age-induced diabetes in mice. *Cell metabolism*, 14(4), 528-536.
- Yosef, R., Pilpel, N., Tokarsky-Amiel, R., Biran, A., Ovadya, Y., Cohen, S., ... & Ben-Porath, I. (2016). Directed elimination of senescent cells by inhibition of BCL-W and BCL-XL. *Nature communications*, 7.
- Yu, A., Zheng, Y., Zhang, R., Huang, J., Zhu, Z., Zhou, R., ... & Yang, Z. (2013). Resistin impairs SIRT1 function and induces senescence-associated phenotype in hepatocytes. *Molecular and cellular endocrinology*, 377(1), 23-32.
- Zindy, F., Eischen, C. M., Randle, D. H., Kamijo, T., Cleveland, J. L., Sherr, C. J., & Roussel, M. F. (1998). Myc signaling via the ARF tumor suppressor regulates p53-dependent apoptosis and immortalization. *Genes & development*, 12(15), 2424-2433.